

**COMPARISON OF PHYSICAL AND
CHEMICAL PROPERTIES OF FIVE
DIFFERENT ALLOPLASTIC BONE
GRAFT MATERIALS**

DISSERTATION

**Submitted to The Tamil Nadu Dr MGR Medical
University In the partial fulfillment
of the requirement for the
Degree of Master of Dental Surgery**




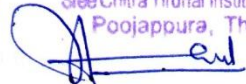
**BRANCH II
PERIODONTOLOGY
2010 - 2013**

Certificate

Certified that the dissertation entitled “**COMPARISON OF PHYSICAL AND CHEMICAL PROPERTIES OF FIVE DIFFERENT ALLOPLASTIC BONE GRAFT MATERIALS**” is a bonafide record of the work done by **Dr.Mintu M Kumar** under our guidance during her post graduate study during the period of 2010-2013 under THE TAMIL NADU Dr. MGR MEDICAL UNIVERSITY, CHENNAI, in partial fulfillment for the degree of MASTER OF DENTAL SURGERY IN PERIODONTOLOGY, BRANCH II. It has not been submitted (partial or full) for the award of any other degree or diploma.


Dr. Elizabeth Kosfi M.D.S.
Professor & Head
Dept. of Periodontics
Sree Mookambika Institute of Dental Sciences
Kulasekharam


DR. ARUN SADASIVAN MDS
PROFESSOR, DEP OF PERIODONTICS
SREE MOOKAMBIKA INSTITUTE OF DENTAL SCIENCE
KULASEKHARAM - 629161

Dr. P.R. HARIKRISHNA VARMA Ph.D.
Scientist in Charge, Bioceramics & SEM Laboratories
Biomedical Technology Wing
Sree Chitra Tirunal Institute of Medical Sciences and Technology
Poojappura, Thiruvananthapuram-695 012


Dr. Elizabeth Koshi

Professor and Head

Dept. of Periodontics,

Sree Mookambika Institute

of Dental Sciences,

Kulasekharam

Dr. Arun Sadasivan (Guide)

Professor,

Dept. of Periodontics,

Sree Mookambika Institute

of Dental Sciences,

Kulasekharam

Dr.P.R.Harikrishna Varma(Co-Guide)

Engineer F,

Biomedical Technology Wing,

Sree Chitra Tirunal Institute of

Medical Science & Technology,

Thiruvananthapuram



ACKNOWLEDGEMENT

I pray to God, who has been more than generous and kind to me to instill these qualities in all of us and make us better medical professionals.

I thank God for endowing me with a wonderful teacher, **Dr. Elizabeth Koshi MDS**, Professor & Head, Department of Periodontics, Sree Mookambika Institute of Dental Sciences who has been very helpful and kind to me.

I take this opportunity to thank and express my gratitude to my Guide **Dr. Arun Sadasivan MDS**, Professor who has been very encouraging and whose constant support has really helped me to complete my study.

I am most grateful to my co – guide **Dr.P.R.Harikrishna Varma**, Engineer F, SCTIMST, Trivandrum whose knowledge and experience in the field of biomaterials made my study a reality.

I would like to acknowledge the help and support given by **Dr.Velayuthan Nair MBBS, MS** Chairman and **Dr. Rema V Nair MBBS, MD, DGO** Director Sree Mookambika Institute of Dental Sciences without which my study would not have been possible.

I would like to thank **Dr. Prabakar C S, Dr Arunima P R, Dr Rajeev A and Dr Nita Syam**, without whom my study would not have been completed.

It's my utmost privilege to acknowledge the debt I owe to the staff members of Bioceramics & SEM Laboratories, Sree Chitra Tirunal Institute of Medical Science & Technology, Thiruvananthapuram especially **Mr. Suresh Babu, Mr. Nishad, Mr**

Vijayan, Mrs. Radha Kumari and **Mr. Moses** for their technical help, constant encouragement and liberty they provided me during the course of this study.

I am deeply indebted to IFGL private limited and Nova Bone Products Limited, USA for providing me with the necessary material, which were used in this study.

I am thankful to my colleagues **Dr Gayathri.S, Dr Shubha Rani, Dr Menaka** and **Dr Arya** for their help and encouragement through my study works.

I am thankful to my husband **Dr. Sarath. C**, for his encouragement, appreciation and support all through my study works.

I also thank my parents, sister and my dear friends who have not only been my pillars of strength but also shoulders that I could lean and weep on in times of despair.

CONTENTS

SL NO	INDEX	PAGE NO
1.	List of Abbreviations	I
2.	List of Tables	II
3.	List of Colour Plates	III-IV
4.	Abstract	V-VII
5.	Introduction	1-7
6.	Aims & Objectives	8
7.	Review of Literature	9-33
8.	Materials & Methods	34-44
9.	Results and Observations	45-65
10.	Discussion	66-73
11.	Summary & Conclusion	74
12.	Bibliography	VIII-XIV

LIST OF ABBREVIATIONS

SEM	Scanning Electron Microscope
TG / TGA	Thermogravimetry / Thermogravimetric Analysis
FTIR	Fourier Transform Infrared Spectroscopy
IR	Infrared Spectroscopy
XRD	X-Ray Diffractometry
JCPDS	Joint Committee on Powder Diffraction and Standards
ICP-OES	Inductively Coupled Plasma Optical Atom Emission Spectroscopy
HA	Hydroxy Apatite
TCP	Tri-Calcium Phosphate
HT	Hydroxy apatite – Tricalcium phosphate combination
PG	Perio Glas
HABG	Hydroxy Apatite Bio-Active Glass Combination

LIST OF TABLES

Table 1	Particle size by SEM – at low magnification of 100x
Table 2	Pore size by SEM – at high magnification of 6000x
Table 3	Crystal size by Scherrer equation from XRD data
Table 4	Percentage of crystallinity

LIST OF COLOR PLATES

- CP1a ESEM – Environmental Scanning Electron Microscopy
- CP 1b SEM connected to computer
- CP 2 Thermogravimetry machine in closed position
- CP 3 Alumina crucibles
- CP 4 Thermogravimetry machine in open position
- CP 5 Crucible loaded
- CP 6 FTIR machine in open position
- CP 7 FTIR machine in closed position
- CP 8 Hydraulic pellet press by PCI services
- CP 9 Hydraulic pellet press by Perkin Elmer
- CP 10 Agate mortar and pestle
- CP 11 Test material placed in a die
- CP 12 Die in closed position
- CP 13 Die placed in pellet press
- CP 14 Pressure raised to 1000psi
- CP 15 Pellet obtained
- CP 16 Pellet placed in FTIR machine
- CP 17 Passage of infra red rays
- CP 18 Results seen as graph in computer
- CP 19 XRD machine
- CP 20 XRD machine – close up view
- CP 21 Agate mortar and pestle for grinding
- CP 22 Thermal vacuum machine

- CP 23 Prepared TrisHCl buffer
- CP 24 Magnetic stirrer
- CP 25 pH meter
- CP 26 ICP machine
- CP 27 Machine for deionised water preparation

Abstract

AIMS AND OBJECTIVES

The present study aims at analysing physicochemical characteristics of 5 different types of alloplastic graft materials used in periodontal regeneration.

MATERIALS AND METHODS

The materials used were:- Monophasic Hydroxyapatite – Biograft HA, Tricalcium Phosphate – Biograft TCP, Biphasic Hydroxyapatite – Biograft HT, Bioactive Glass – Perioglas and a combination of Hydroxyapatite and Bioactive Glass – Biograft HABG Active.

MATERIAL CHARACTERIZATION

The physicochemical properties of the biomaterials were tested using the following methods:

1. Scanning Electron Microscopy [SEM] - assess the sample's surface topography & size
2. Thermogravimetry - reflect divergent physical properties and chemical compositions among the specimens resulting from their diverse thermal histories.
3. Fourier Transform Infrared Spectroscopy [FTIR] - to provide information concerning the chemical composition and the major functional groups.
4. X ray diffractometry [XRD] - used to identify phase and composition features and qualitatively evaluate the crystallinity of the materials
5. Dissolution rates - used to evaluate the solubility rate of calcium and silica

RESULTS

From the particle size related data it is seen that PG and HA show smaller particles (100 – 300 μm) while TCP, HT and HABG show larger particles (200 – 500 μm). In the present study Biograft HA, Biograft TCP and Biograft HABG showed rough and irregular surface, while Perioglas and Biograft HT showed a smooth surface. The surface of perioglas

is said to be smooth with less roughness, Biograft HT shows smooth and sintered surface particles with nano pores visible. All the other materials show rough surface with the presence of micro and nano sized pores ranging from 0.5 – 1 μm . Thermogravimetric analysis is used to determine the content of water, organic material (like collagen) and mineral (CaP). For all of the alloplasts in our study only a minimal weight loss upto 2 % was seen which can be attributed to the presence of moisture or due to oxidation of the samples. As all the test materials were synthetic or alloplastic, there was the absence of lattice water or organic content. All the tested materials were stable upto 1000⁰ C, which renders all test materials to be thermally stable and phase pure and without any impurities. Infra red analysis shows the presence of main functional groups such as phosphates and carbonates. The calcium phosphate class of materials (HA, TCP and HT) and HABG showed almost similar stretching and vibration patterns for both functional groups. Phosphate peak was broad in Perioglas which may be due to the amorphous nature of material. In the Infrared spectra data from the 5 tested materials, hydroxyl peaks had highest intensity in HA, with midway values in HT and almost nil in TCP. HABG does not show a peak corresponding to OH group and PG shows a broadened peak. X ray diffraction patterns of the 5 alloplastic materials indicate their chemical composition (presence of crystalline phases) and lattice parameter information. The XRD peaks of the samples were well defined. Among the 5 alloplastic materials HA, HABG, TCP and HT showed typical crystalline structure whereas PG showed broad peaks indicating the amorphous nature of the material. An increasing order of crystallinity was obtained from XRD data as PG, HABG, TCP, HT and HA. In the dissolution tests done for calcium, all the materials showed positive results. Bioactive glass class of grafts (PG and HABG) had more dissolution when compared to hydroxyapatite class (HA, TCP and HT). The second dissolution test was done for silica, the bioactive glass group of material (PG and HABG) which are silica based were tested. Both PG and HABG showed increased

dissolution of silica upto 24 hours, with PG showing constant values and HABG showing decreasing rates after 24 hours.

SUMMARY

The main objective of present work was the physicochemical characterization of 5 commercial sample of alloplasts used for bone grafting. The alloplastic biomaterials belonged to 3 main classes calcium phosphate group (HA, TCP and HT), bioactive glass group (PG) and a combination graft (HABG). However even for those with similar chemical characteristics, significant differences were noted with regard to particle size, porosity, surface roughness, presence of functional groups, crystallinity and dissolution properties. Among the materials tested calcium phosphate based ceramics and bioactive glass – ceramic combination showed porous surface architecture parameters conducive to cellular and vascular proliferation. Thermogravimetric analysis revealed that all the materials were phase pure with no impurities. Infra red spectrometry showed presence of functional groups essential for bone integration in all test materials with Perioglas and Biograft HABG showing presence of silica which has a beneficial effect in bone formation. X ray diffractometric analysis revealed that with the exception of Perioglas which was amorphous all the other materials were crystalline in nature. Increased dissolution of calcium and silica were seen in bioactive glass group when compared with calcium phosphate and mixed calcium phosphate grafts

Introduction

The periodontium consists of the investing and supporting tissues of the tooth.¹ The periodontium encompasses the alveolar bone, root cementum, periodontal ligament and gingiva.² The gingiva gives protection to the underlying tissues and the attachment apparatus is composed of the periodontal ligament, cementum and alveolar bone.¹ The mineralized or hard connective tissues are alveolar bone and cementum while the fibrous or soft connective tissues are periodontal ligament and the lamina propria of the gingiva. The periodontal ligament is the soft connective tissue between the two hard connective tissues of the periodontium.³

The main function of the periodontium is to attach the tooth to the bone tissues of the jaws and to maintain the integrity of the surface of the masticatory mucosa of the oral cavity. The periodontium anchors the roots of the teeth to the bones of jaw and thus provides support during mechanical stress and trauma.⁴ The periodontium constitutes a developmental, biologic and functional unit which undergoes certain changes with age and alterations in the oral environment. The human oral cavity is colonized by a large number of highly diverse bacteria existing in either a planktonic community or in a complex sessile community known as a biofilm(dental plaque). While the majority of bacteria in these complex communities are nonpathogenic some bacteria are opportunistic pathogens and are associated with extraoral and intraoral diseases. Plaque biofilm begins to develop immediately after a tooth surface is mechanically cleansed and increases both in amount and complexity over time. Presence of specific microorganisms in both supra- and subgingival biofilms are associated with three common chronic intraoral inflammatory diseases; caries, gingivitis and periodontal diseases. Gingivitis is an inflammatory disease that is associated with proliferation of local epithelial cells and loss of gingival connective tissues but is not associated with loss of connective tissue attachment. The most

common form of gingivitis occurs due to the accumulation of biofilm on teeth. The undisrupted biofilm or “neglected” gingivitis is said to be the most common form of periodontal disease and is experienced by all individuals at some time.

Periodontal diseases are among the most prevalent diseases in humankind.⁵ The initial lesion of the periodontium is gingivitis which can (but not always), lead to periodontitis.⁶ Periodontal disease is a multifactorial disease and consists of closely related diseases which vary in etiology, natural history and response to therapy. However, plaque is considered to be the main etiologic factor. Chronic periodontitis is an infectious disease resulting in inflammation of the periodontium and is characterized by pocket formation and or / gingival recession. It is reasonable to understand that the disease will progress if further if treatment is not provided². Its clinical features include symptoms like alteration in color, texture and volume of marginal gingiva, bleeding on probing from gingival pocket area, reduced resistance of the soft marginal tissues to probing, loss of probing attachment level, recession of gingival margin, loss of alveolar bone, root furcation exposure, increased tooth mobility, drifting and eventually exfoliation of teeth.⁷

Therapeutic modalities should therefore aim not only at eliminating the gingival inflammatory process and preventing the progression of periodontal disease but also at re establishing and regenerating the periodontal tissue previously lost to the disease⁸. Periodontal treatment requires an interrelationship between the care of the periodontium and other phases of dentistry.¹ The concept of total treatment is based on the elimination of gingival inflammation and the factors that lead to it. Total treatment requires consideration of systemic aspects, including the possibility of interaction of periodontal disease with other disease, systemic adjuncts to local

treatment and special precautions in patient management necessitated by systemic conditions. Periodontal treatment traditionally comprises initial nonsurgical debridement followed by a re evaluation, at which stage the need for further treatment, usually surgical in nature, is established.⁷ Nonsurgical mechanical periodontal treatment is the cornerstone of periodontal therapy and the first recommended approach to the control of periodontal infections.⁹

Nonsurgical therapy for the control of periodontitis normally consists of subgingival debridement combined with oral hygiene instruction. Re-evaluation of results following initial treatment is critical for adequate selection of additional therapy and for establishing the best possible longterm prognosis. The purpose of surgical pocket therapy is to eliminate the pathologic changes in the pocket walls, to create a stable, easily maintainable state and to promote periodontal regeneration.¹ Pocket elimination was considered to be a desirable treatment outcome, giving rise to the gingivectomy and apically repositioned flap techniques.¹⁰

Regeneration is defined as the reproduction or reconstitution of a lost or injured part, with form and function of lost structures restored. Periodontal regeneration includes regeneration of alveolar bone, cementum, periodontal ligament and gingival.¹¹ Periodontal defects may be morphologically characterised as suprabony or intrabony, as furcation or gingival recession defects or their combinations. Regeneration of the lost periodontium is one of the main goals of periodontal therapy. Conventional periodontal treatments, such as scaling and root planing are highly effective at repairing disease-related defects and halting the progression of periodontitis. However, they do little to promote regeneration of the lost periodontium.¹² On the other hand, periodontal surgery in particular regenerative

periodontal surgery aims not only to eliminate pocket depths, but to regenerate a new attachment apparatus and reconstruct the periodontal unit to within previously existing normal physiologic limits. Regenerative materials include non bone graft associated new attachment and bone graft associated new attachment. Some non bone graft associated new attachment techniques include curettage, excisional new attachment procedure, guided tissue regeneration, biomodification of the root surface, biologic mediators and enamel matrix proteins. Bone graft materials include autografts, allografts, xenografts and alloplasts.¹

Bone grafting is possible because bone tissue, unlike most other tissues, has the ability to regenerate completely if provided the space into which to grow. As native bone grows, it will generally replace the graft material completely, resulting in a fully integrated region of new bone. The objectives of periodontal bone grafts include probing depth reduction, clinical attachment gain, bone fill in the osseous defect and regeneration of new bone, cementum and periodontal ligament.¹³ The ideal bone graft material should be able to trigger osteogenesis, cementogenesis, and a functionally oriented periodontal ligament at a more coronal level of attachment to the root surface. Bone graft materials are generally evaluated based on their osteogenic, osteoinductive or osteoconductive potential. Osteogenesis, the formation of mineralized bone by osteoblasts, is achieved only with autogenous grafts. ie the formation or development of new bone cells contained in the graft. Osteoinduction in the graft convert the neighbouring cells into osteoblasts, which in turn form bone. Osteoconduction is a physical effect by which the matrix of the graft forms a scaffold that favors outside cells to penetrate the graft and forms bone. Here, the bone substitutes do not provide any cellular elements. Most of the bone substitutes are osteoconductive, inert filling materials and integrate with new bone.¹⁴

Autografts have been considered the ideal bone grafting material in bone reconstructive surgery due to its osteogenic, osteoinductive and osteoconductive properties. Autografts can include cortical, cancellous or cortico – cancellous bone from both intraoral or extraoral sites.¹⁵ Common donor sites are maxillary tuberosity and other edentulous alveolar areas like healing extraction sockets or osseous coagulum harvested during osteoplasty procedures. Other areas like mental and mandibular retromolar areas may also be used. Extra oral sites may include sites like tibia, iliac crest and ribs. Mostly, sufficient autogenous bone is unavailable or harvesting would require additional surgical sites, increased patient morbidity and clinical chair time.¹⁶ There are other limitations like increased operative time, wound complications, local sensory loss and chronic pain.¹⁷

Allografts are graft materials obtained from another individual of the same species. Allografts are commercially available from tissue banks. They are obtained from cortical bone within 12 hours of death of the donor, defatted, cut in pieces, washed in absolute alcohol and deep frozen. The material may then be demineralised, and ground, sieved to a particle size of 250-750 um and freeze dried and vacuum sealed in glass vials.¹ Allografts have the same characteristics as autografts but lack osteogenic cells. It has osteoinductive properties but may not be recognized unless demineralised.¹⁸ Allogenic bone grafts from a different person may cause disease transmission. Also complications like fracture, non union and infection will be present.

Xenografts are grafts taken from another species. It is also called heterograft.¹⁹ Xenografts are osteoconductive, readily available and has a risk of disease transmission. Disease transmission and permanent alteration to the genetic code of

animals were of concern. This has driven to the development of alloplastic graft materials.¹⁶

Alloplastic bone substitutes represent a large group of chemically diverse synthetic calcium – based biomaterials like calcium phosphate, calcium sulphate, bioactive glasses and polymers.¹⁵ Ceramics, collagen and polymers are the most recently used alloplastic materials, they can be either bioactive or bioinert. Bioactive ceramics include hydroxyapatite, fluorapatite, bioglass and tricalcium phosphate. They may be porous or non porous.²⁰ Depending on how it is made, it may be "resorbable" or "non-resorbable". The 1996 World Workshop in Periodontics has concluded that synthetic graft materials function primarily as defect fillers. Several alloplastic implant materials have been used in an attempt to improve clinical conditions and regenerate bone in periodontal infrabony defects.

Alloplasts are broadly defined as synthetic implantable biomaterials. They are widely available in different forms in terms of density, porosity and crystallinity, all of which are engineered into the product. Biocompatibility and tissue response to alloplast materials is excellent, and there is no risk of disease transmission associated with their use. Their mechanism of action is via osteoconduction. Alloplasts may be used alone as osteoconductive scaffolds, or more commonly as volume expanders in combination with freeze-dried or autogenous bone as a "composite" graft. Implantation of a graft material, whether natural or synthetic, results in a host response. There are effects at the tissue, cellular, and molecular level resulting from the interaction of the host tissue with the implanted material. These effects are chiefly dependent on the morphology, chemical composition, porosity and particle size of the material.

Alloplastic bone substitutes represent a large group of chemically diverse synthetic calcium based biomaterials like calcium phosphate, calcium sulphate, bioactive glasses and polymers, ceramics, collagen and polymers are the most recently used alloplastic materials. They can be either bioactive or bioinert, porous or non-porous and depending on how it is made, it may be resorbable or non-resorbable. The various alloplasts used in the present study include Monophasic Hydroxyapatite (Biograft HA), Biphasic Hydroxyapatite which contains Hydroxyapatite and Tri Calcium Phosphate (Biograft HT), Tricalcium Phosphate (Biograft TCP), Bioactive Glass (PerioGlas) and a Combination of Hydroxyapatite and Bioactive Glass (Biograft HABG Active). Based on the chemical composition and physical characteristics of these alloplastic materials, their biological performance differs. The present study is aimed at evaluating these physical and chemical characters by Scanning Electron Microscopy [SEM] to assess the sample's surface topography, composition, porosity etc, Thermogravimetry [TG] to identify the divergent physical properties and chemical compositions among the specimens resulting from their diverse thermal histories, Fourier Transform Infrared Spectroscopy [FTIR] to provide information concerning the chemical composition and the major functional groups, X ray diffractometry [XRD] is used to identify phase and composition features and qualitatively evaluate the crystallinity of the materials and dissolution rates to find the solubility rate of calcium and silica from the materials tested.

The present study was designed to compare the physicochemical properties of alloplastic bone graft materials used in periodontal regenerative procedures in order to acquire a full interpretation of the in vivo performance of the materials.

Aims & Objectives

AIMS & OBJECTIVES

The purpose of the present study is to evaluate the physicochemical characteristics of 5 different alloplastic graft materials which include Biograft HA, Biograft HT, Biograft TCP, PerioGlas and Biograft HABG Active by using various analytical methods including Scanning Electron Microscopy [SEM], Thermogravimetry[TGA], Fourier Transform Infrared Spectroscopy [FTIR], X ray diffractometry [XRD] and Dissolution rates.

Review of Literature

STUDIES ON SCANNING ELECTRON MICROSCOPY

Fabbri et al 1995²¹ suggested a method to obtain a substrate of high porosity, exploiting the impregnation of spongy substrate with hydroxyapatite ceramic particles. Scanning electron microscopy and optical microscopy images were used to ascertain the porosity characteristics. Optical microscopy observations show a texture similar to that of bone, having very diversified walls with respect to both internal and external shape and geometry. An open porosity with interlinked pores is assured. Through scanning electron microscopy examinations, it was possible to ascertain the architecture in a wider field and at higher magnifications.

Best et al 1997²² evaluated the physical and chemical characters of two synthetic hydroxyapatite powders (A and B), supplied by different manufacturers in the as-received condition and after heat treatment at 1250 °C for 4 h. The morphology of powders was studied with a JEOL 6300 scanning electron microscope with an accelerating voltage of 20 kV. Powder samples were attached to double-sided adhesive carbon tape on a brass stub and sputter coated for approximately one minute using a gold/palladium target. Scanning electron microscopy of the two powders indicated that powder A appeared to be composed of hard agglomerates of acicular crystallites and that powder B consisted of larger, angular porous agglomerates of spheroid particles approximately 0.5 µm in diameter. Intergranular, surface porosity was more evident in material B than in material A, but the surfaces of both materials showed mixed areas of high density and regions of higher porosity. The mean grain size of material B was found to be slightly higher than for material A, but was retained at approximately 2 µm indicating that no accelerated grain growth had taken place.

Joschek et al 2000²³ obtained porous hydroxyapatite ceramics derived from bovine bone (Endobon) from Merck, Darmstadt, Germany. Granules from eight

different batches with grain sizes between 2.8 and 5.6 μm were used for investigations. The samples were mounted on aluminum SEM pins and sputter coated with Au/Pd using a sputter coater (model SCD 040 from Balzers, Balzers, Liechtenstein). They were investigated with a digital scanning electron microscope (DSM 940, Zeiss, Oberkochen, Germany) at magnifications between 20x and 5000x using acceleration potentials between 10 and 15 keV. It was seen that Endobon is produced from a natural material. The ceramic has an interconnecting pore system with pores of sizes 0.1-500 μm which is similar to the natural structure of bone and is preserved during manufacturing. The size of the hydroxyapatite crystals ranges from 1 to 7 μm which was 2-3 times larger than natural bone.

Pilliar et al 2001²⁴ studied the porous structure formed by gravity sintering calcium polyphosphate (CPP) particles of either 106-150 or 150-250 μm size to form samples with 30-45 vol% porosity. Sintered disk samples were examined using scanning electron microscopy to determine pore size and shape, inter-particle sinter & neck junction dimensions, as well as to assess microstructural features such as the structure of the crystals (grains) making up the individual CPP sintered particles. To determine porosity, sintered samples of each powder size were embedded in polymethylmethacrylate, cross-sections cut using a diamond wafering blade and the cut surfaces polished to 1200 grit silicon carbide paper finish. Polished sections were prepared both parallel and normal to the initial long axis of the sintered rods. The coarse powder samples appeared less dense. Extensive neck formation occurred during sintering for both the fine- and coarse-powder sintered samples.

Porter et al 2003²⁵ studied the incorporation of silicate into hydroxyapatite (HA) which was previously shown to significantly increase the rate of bone apposition. After preparation, powders and granules of HA and Si-HA were sintered

at 1200°C for 120 min using a ramp rate of 2.5°C/min. These granules were dispersed onto the surface of aluminium stubs and subsequently sputter coated with 10 nm of gold. Scanning electron microscopy in secondary electron mode was performed in a Phillips XL30 FEG operated at 5 kV, using a 30 µm thin foil final aperture. Irrespective of their chemical composition, Scanning Electron Microscopy of HA and Si -HA shows similar morphology of the granules.

Tadic and Epple 2004²⁶ studied fourteen different bone substitution materials without any treatment, except for grinding or cutting to a size appropriate for analysis. Scanning electron microscopy was carried out using a LEO 1530 instrument on gold-sputtered samples. Bioresorb, Chronos, Ceros, Cerasorb, Vitoss, PepGen, Algipore, BioOss, and Tutoplast were available as granulate with particle sizes of a few hundred µm to a few millimeters. Ostim was a fluid paste with nanoscopic apatite particles in aqueous dispersion. Cerabone, Endobon, and Tutoplast had the bone-like structure with interconnecting porosity as they were all derived from natural bone by either thermal or chemical treatment while blocks of Cerasorb were prepared by cold isostatic pressing, followed by mechanical drilling of millimeter-sized holes. Cerasorb showed the granular appearance of a sintered material with visible micropores at high magnification. The calcined bovine bone Cerabone had the interconnecting porous structure of the original bone. The chemically converted structure of Algipore was seen. Tutoplast with interconnecting macroporosity of bone was seen.

Luna Zaragoza et al 2009²⁷ evaluated the chemical and surface properties of calcium and iron phosphates as the first stage in an investigation of their use as reactive materials to absorb metal ions from aqueous solutions. A bovine femur obtained from a slaughterhouse was cleaned, cut, milled, and washed with deionized water and hydrogen peroxide in water. Fat was removed from the bone particles,

which were then annealed at 960°C for 24 hours. The annealed bone particles were then centrifuged 3 minutes with deionized water and then washed with phosphoric acid at 2.3 pH. The morphology of the iron and calcium (bovine bone) phosphates was analyzed in a Phillips XL-30 scanning electron microscope at 25kV. The samples were mounted on an aluminium holder with carbon conductive tape, and covered with a gold layer approximately 200 Å thick using a Denton Vacuum model Desk II sputter coater. Since once the bone was annealed, the organic matter transformed into gases (mainly CO₂) and there were holes seen due to loss of this organic matter. These pores seem to be connected by solid walls to form separated continuous networks with a surface texture varying from rough to smooth. At 4000x, the surfaces of the bone that are not seen to be porous at low amplification show smaller pores, although these particles do not show agglomerates.

Sena et al 2009²⁸ studied a composite of hydroxyapatite (HA)-type I collagen (Col) as a tissue-engineered bone graft which could act as a carrier or a template structure for cells or any other agents. HA/Col composites with HA:Col weight ratios of 80:20; 50:50; 20:80, and 10:90 were produced by the aqueous precipitation method, using a native Type I Col gel. The samples were mounted on aluminum stubs using double-sided carbon tape, were sputter-coated with a thin layer of gold to avoid electrical charging, and observed after the application of 15 kV of accelerating voltage. This was done for morphologic evaluation using SEM. It was observed that a large amount of calcium phosphate (CaP) precipitate on the HA/Col 80/20 composite fibers. A significant amount of CaP was poorly adhering to the Col surface and became loose while manipulating the composites. As for the HA/Col 50/50 composite, apatite seems to be more strongly attached, and no particle detachment was observed during the manipulation process. The apatite crystals are homogeneously distributed

within the Col fibers in the 20/80 HA/Col composite. However, in the 10/90 HA/Col composite, the high concentration of Col hinders the dispersion of the fibers during their formation, causing an agglomeration of particles linked with native Col fibers.

Laura Floroian 2010²⁹ evaluated a new bioactive glass composition for medical applications by the addition of fluorides, such as CaF₂ and MgF₂, for the substitution of Na₂O in the conventional bioactive glass composition. Microstructures were observed with a FE-SEM (JSM- 7500F, JEOL, Japan). The microstructure of BG1 shows the hydroxyapatite phase composed of small particle groups homogeneously distributed in the matrix. Large particles with a plate shape were observed only in the BG2 sample. In the microstructures of BG5, BG8 the hydroxyapatite phase was revealed with crystals homogeneously distributed in the matrix.

Goudori et al 2011³⁰ investigated the in vitro bioactivity of sol-gel derived DC/BG composites as powders and as disk shaped heated specimens in periodically renewed SBF. The in vitro bioactivity of the composites (powders and specimens) was tested for various immersion times in c-SBF solution that was renewed after 6 h, 24 h and then every 2 days, as proposed by Zhong and Greenspan. Topographical evaluation and surface elemental compositions of the samples after being carbon coated were performed with a scanning electron microscope with associated EDS (JEOL J.S.M. 840A, Tokyo, Japan). SEM microphotographs revealed no significant alteration of the surface of the specimens for both DC/BG composites after 9 days of immersion. On the contrary after 18 days the surfaces of all specimens are fully covered by a well structured apatite layer consisting of spherulitic aggregates.

Rezakhami et al 2012³¹ studied different nanocrystals of hydroxyapatite-[HAp]-gelatin [GEL], HAp/GEL/Glutaraldehyde (GA), HAp/GEL/Zn and

HAp/GEL/GA/Zn were prepared using the biomimetic process and were characterized. The slurry for HAp/GEL composite was prepared by the simultaneous titration method. The morphologies of the products were observed through scanning electron microscopy (SEM, Cambridge S365). When HAp/GEL/Zn nanocrystal is sintered to 900°C, the morphology of HAp particles is clearly rod shape.

STUDIES ON THERMOGRAVIMETRIC ANALYSIS

Peters et al 2000³² combined thermogravimetry±differential thermal analysis ±mass spectrometry using a Netzsch STA 409/Balzers QMS 421 system (sample mass: 71 to 91 mg; open alumina crucibles; 30±1000°C; 10 K min⁻¹; dynamic air atmosphere; 50 ml min⁻¹). The sample losses were weighed in three steps. The first step occurs from 50 up to about 260°C (water; signal at m/z.18). In the second step, up to about 600°C, the organic components (bone marrow, fat tissue, collagen) are pyrolyzed and burnt (combustion products water and carbon dioxide, m/z.44, and organic fragments, e.g. methyl, m/z.15). In the third step, between 650 and 850°C, carbon dioxide released from carbonated apatite is detected.

Suchanek et al 2002³³ prepared crystalline carbonate- and sodium-and-carbonate-substituted hydroxyapatite (CO₃HAp and NaCO₃HAp) powders at room temperature via a heterogeneous reaction between Ca(OH)₂/CaCO₃/Na₂CO₃ and (NH₄)₂HPO₄ aqueous solution using the mechanochemical hydrothermal route. Thermogravimetric analysis (model TGA-6, Perkin Elmer Co., Norwalk, CT) was performed in air at a flow rate of 20 ml/min. Samples were heated to a maximum temperature of 950°C using a heating rate of 5°/min. Significant loss of weight was observed up to approximately 450°C for all samples and was due to the loss of adsorbed (up to ≈120°C) and lattice water. Another significant and gradual weight loss of CO₃HAp powders occurred above 550°C, which is attributed mostly to the

loss of carbonate with subsequent formation of CaO. In all the powders, a significant loss of weight was observed up to approximately 450°C and was due to the loss of adsorbed and lattice water. Another weight loss for NaCO₃HAp powders occurred above 550°C and was attributed mainly to the loss of carbonate with subsequent formation of Na₂O and CaO. No weight losses related to the decomposition of Na₂CO₃ (around 400°C), Ca(OH)₂ or CaCO₃ were observed, which in addition to the XRD data serves as evidence that the as-prepared powders were phase pure NaCO₃HAp.

Tadic and Epple 2004²⁶ characterised fourteen different synthetic or biological bone substitution materials using high-resolution X-ray diffractometry, infrared spectroscopy, thermogravimetry, and scanning electron microscopy. The biological performance of a synthetic material depends on fundamental parameters: chemical composition, morphology, and biodegradability. Thermogravimetric analysis (TGA) was carried out with a TG/DTAS II, Seiko Exstar 6000 instrument (5–15 mg; 25 – 1000°C; 10Kmin⁻¹; dynamic oxygen atmosphere; 300 ml min⁻¹; Al₂ O₃ crucibles). From room temperature to about 200°C, incorporated water is lost. Above about 300°C, organic material like collagen, fat tissue, proteins start to burn. At about 400°C, only the mineral phase is left. If the mineral contains some carbonate in the form of carbonated apatite, there is a mass loss between about 400°C and 900°C. Thus, it was possible to find the mineral content and carbonate content of the materials tested.

Suchanek et al 2004³⁴ prepared magnesium-substituted hydroxyapatite powders with different crystallinity levels at room temperature via a heterogeneous reaction between Mg(OH)₍₂₎ /Ca(OH)₍₂₎ powders and an (NH₄)₍₂₎ HPO₍₄₎ solution using the mechanochemical-hydrothermal route. A small quantity of each purified

Mg-HAp powder was placed in an alumina crucible and heat treated in air at 900°C for 1 h with a heating rate of 10°C/min (rapid temperature furnace, CM Inc., Bloomfield, NJ). In all the powders, significant loss of weight up to approximately 450°C was very likely due to the loss of adsorbed and lattice water. Loss of the carbonate ions could contribute to the total weight loss above 550°C. HPO_4^{2-} groups, which are incorporated into HAp lattice together with Mg transform into pyrophosphate in the temperature range of 400–700°C with a formation of water. Above 600–700°C, nonstoichiometric Mg-HAp decomposes, usually with the formation of whitlockite and water.

Susan et al 2005³⁵ prepared nanocarbonated hydroxyapatite/ collagen composite via biomimetic self assembly method. The carbonated weight percentages were measured through TGA by Rigaku Thermoflex TG8110/TAS100. Samples were heated from room temperature to a maximum temperature of 1000°C in increments of 10°C/min. Three stages of weight loss is seen: to determine content of water, organic material, carbonated apatite and mineral left.

STUDIES ON INFRA RED SPECTROSCOPY

Best et al 1997²² physically and chemically characterized two synthetic hydroxyapatite powders (A and B), supplied by different manufacturers, in the as-received condition and after heat treatment at 1250°C for 4 h. Fourier transform infrared (FTIR) spectra were obtained using a Nicolet 800 spectrometer in conjunction with a MTech photo-acoustic (PAS) cell. Spectra were obtained at 4 cm^{-1} resolution averaging 128 scans. Infrared spectroscopy results both for the asreceived powders and after sintering showed that the materials contained traces of carbonate. There was a broad band shouldered on the OH peak and no disruption in the phosphate bands indicating that the material was hydroxylated. However, the OH

peaks in powder B were of a higher intensity than those of powder A. After sintering, the carbonate peaks and the OH peaks at 3600 cm^{-1} in both materials decreased slightly in intensity.

Peters et al 2000³² studied bone samples of different origins and two bone substituent materials with modern solid-state chemical method. Fourier transform IR-spectroscopy was carried out with a Perkin±Elmer PE1720 instrument in KBr pellets. The results from IR spectroscopy show that endobon is well crystallized whereas natural bone samples and Kiel bone contain disordered crystallites. The carbonate and organic tissue can be detected as well. Endobon and hydroxyapatite are highly crystalline, as shown by the band-splitting at $1030\pm 1100\text{ cm}^{-1}$. Kiel bone, tumor bone and callus bone contain hydroxyapatite with medium crystallinity. The carbonate content appears to be higher in Kiel bone and tumor bone as compared to callus bone. In spongiosa B, the vibration bands of apatite are barely visible.

Suchanek et al 2002³³ studied carbonated apatite powders. Infrared spectra of all batches of as-prepared CO_3HAp and NaCO_3HAp powders were obtained using an infrared Fourier-transform spectrometer (FTIR, model 1720-X, Perkin Elmer Co., Norwalk, CT). For this purpose, each powder was mixed with KBr in the proportion 1/150 (by weight) for 15 min and pressed into a pellet using a hand press. The FTIR spectra of the as-prepared NaCO_3HAp powders show typical spectra of carbonated HAp ie similar results to those of the CO_3HAp powders. PO_4 -derived bands at 478, 566, 605, 963, and $1030\text{--}1090\text{ cm}^{-1}$, CO_3 -derived bands at 870 cm^{-1} and around $1420\text{--}1480\text{ cm}^{-1}$ and adsorbed water bands at 1630 and $3000\text{--}3700\text{ cm}^{-1}$ were again observed. Very low intensity of both OH-derived bands at 630 and 3570 cm^{-1} , which are clearly visible only in the nominally stoichiometric HAp powder, and broadening of the PO_4 -derived bands with increasing x were observed.

Legeros et al 2003³⁶ prepared a biphasic calcium phosphate bioceramis by a mixture of hydroxyapatite and β tricalcium phosphate of varying HA/ β TCP ratios. The crystallinity of the HA and β TCP phases in BCP depends on sintering temperature of CDA: the higher the sintering temperature, higher the crystallinity. IR revealed the composition of biphasic calcium phosphate but could not determine relative amounts of HA/ β TCP.

Suchanek et al 2004³⁴ prepared magnesium-substituted hydroxyapatite powders with different crystallinity levels at room temperature via a heterogeneous reaction between $\text{Mg}(\text{OH})_2/\text{Ca}(\text{OH})_2$ powders and an $(\text{NH}_4)_2\text{HPO}_4$ solution using the mechanochemical-hydrothermal route. Infrared spectra of all batches of as-prepared and purified Mg-HAp powders were obtained using an infrared Fourier-transform spectrometer (FTIR, model 1720-X, Perkin Elmer Co., Norwalk, CT). For this purpose, each powder was mixed with KBr in the proportion 1:150 (by weight) for 15 min and pressed into a pellet using a hand press. Selected FTIR spectra show bands typical for HAp in addition to a sharp peak derived from OH^- groups in the unreacted $\text{Mg}(\text{OH})_2$ present in the Mg-HAp sample with $x=2.0$. The FTIR spectra exhibit increased broadening of the PO_4^{3-} - derived bands indicating increased structural disorder, which could be caused by increased concentration of Mg in the HAp lattice. These are typical spectra of HAp showing PO_4^{3-} -derived bands at 478, 566, 605, 963, and $1030\text{--}1090\text{ cm}^{-1}$ and adsorbed water bands at 1630 and $3000\text{--}3700\text{ cm}^{-1}$.

Tadic and Epple 2004²⁶ studied fourteen different bone substitution materials without any treatment, except for grinding or cutting to a size appropriate for analysis. Infrared spectroscopy (IR) was carried out with a Perkin-Elmer 1720 instrument (KBr pellet, transmission mode, $400\text{--}4000\text{ cm}^{-1}$, resolution 2 cm^{-1} , 10 scans). All β -TCP

ceramics are identical and show only the expected calcium phosphate bands. The hydroxyapatite based ceramics show only calcium phosphate bands in a sharp and split way, as indicative for the high crystallinity. Algipores shows some carbonate bands (approx. 1400 cm^{-1}) that are probably due to remnants of the production process (from calcium carbonate algae). Although PepGen contains a bioactive peptide, there are no bands of organic material. This is due to the small amount present. The phosphate bands are generally broader because of the small crystallite size. In addition, there are bands of water, and, except for Ostim. This shows that synthetic hydroxyapatite as well as BioOss contain small amounts of incorporated carbonate.

Sena et al 2009²⁸ characterised hydroxyapatite (HA)-type I collagen (Col) composite, a tissue-engineered bone graft which can act as a carrier or a template structure for cells or any other agents. . HA/Col composites with HA:Col weight ratios of 80:20; 50:50; 20:80, and 10:90 were produced by the aqueous precipitation method, using a native Type I Col gel. The composites and HA powder spectra were analyzed by using the Fourier Transform Infrared Spectroscopy (FTIR, Spectra Tech). The chemical groups were then classified into inorganic and organic phases. The presence of impurities such as amorphous calcium phosphate precursors was also evaluated. After that, the data were recorded in a $4000\text{--}400\text{ cm}^{-1}$ spectral range with a 4 cm^{-1} resolution. FTIR analysis did not indicate any alterations in the Col vibration mode for none of the used HA– Col ratios. The spectra of the composites presented characteristic bands of a protein, around $1600\text{--}1700\text{ cm}^{-1}$. This evidences carbonyl stretching at 1560 cm^{-1} and it is associated with amide II vibrations in the plan of the N–H and C–H stretch connection. 1450 cm^{-1} indicates the presence of proline and hydroxyproline pyrrolidine rings.

Goudouri et al 2011³⁰ investigated in vitro bioactivity of sol-gel derived DC/BG composites as powders and as disk shaped heated specimens in periodically renewed SBF. The in vitro bioactivity of the composites (powders and specimens) was tested for various immersion times in c-SBF solution that was renewed after 6 h, 24 h and then every 2 days, as proposed by Zhong and Greenspan. The FTIR transmittance spectra by the KBr pellet technique were obtained using a Perkin-Elmer Spectrometer Spectrum 1000 in MIR region with a resolution of 4 cm^{-1} , the FTIR reflectance spectra were obtained using a Bruker IFS 113v spectrometer in MIR region with a resolution 2 cm^{-1} . The spectra of all powder samples before immersion prove the coexistence of the two constituents in the mixture, by revealing the characteristic bands of both dental ceramic and bioactive glass. The band at 714 cm^{-1} that is assigned to leucite (KAlSi_2O_6 , Lt), which is a dominant phase in dental porcelains, is related to the amount of the dental ceramic in the composite. The enhancement of the double peak at 568 and 604 cm^{-1} on the spectra of all powdered samples, even after 3 days of immersion, is indicative of the onset of apatite formation. The shifting and sharpening of the broad peak at 1100 cm^{-1} attributed to the asymmetric Si-O-Si stretching vibration mode indicates the crystallization of apatite and is only observed after 3, 6 and 9 days of immersion for the 50:50, 60:40 and 70:30 DC/BG composites respectively. Thus, after 9 days the surface of all grains was covered by apatite aggregates.

Greenspan 2011³⁷ studied *IngeniOs* HA Synthetic Bone Particles and Bio-Oss Bone Substitute. A one gram portion of each material was ground to a fine powder using an agate mortar and pestle and then pressed into a KBr pellet for analysis. A Perkin-Elmer Fourier transform infrared spectroscopy (Perkin-Elmer Corp., Waltham, MA, USA) was used to indentify chemical structure by interpreting

the infrared absorption spectrum via the chemical bonds in a molecule. All spectra were collected at room temperature at a nominal resolution of 4.00 and number of sample scans equal to 1000. The FT-IR spectra were recorded in a range of 500-4000 cm^{-1} . Both materials have the signature PO_4 -3 double peak at 550 cm^{-1} and 605 cm^{-1} , although the double peak is much more pronounced in *IngeniOs* HA Synthetic Bone Particles. This is consistent with the broadened XRD spectra and suggests that the crystal structure is more uniform and more crystalline in the *IngeniOs* HA material when compared to the Bio-Oss product. In addition, there is clearly a carbonate peak in the Bio-Oss Bone Substitute (CO_3^{2-}) that is most likely a remnant of the original material, or possibly a result of the processing and thermal treatment of the material. This peak is totally absent in the *IngeniOs* HA material.

Esther et al 2012³⁸ synthesised chlorapatite single crystals using the molten salt method with CaCl_2 as a flux. The samples were analyzed by infrared Fourier spectroscopy (FTIR Bomem, MB-100 series, USA). The spectrum was acquired in the transmission mode, in the range of 400–4,000 cm^{-1} , with a resolution 2 cm^{-1} . To perform the analysis, pellets (containing 100 mg of dry KBr mixed with 1 mg of crushed single crystals) were prepared and vacuum dye pressed. The IR spectrum shows clear bands corresponding to phosphate and the vibration overtones as well as a broad band in the vicinity of 3,400 cm^{-1} due to absorption of water molecules. This analysis can rule out the presence of hydroxyl groups due to the absence of its characteristic vibration bands. A small band with a wave number corresponding to carbonate groups (1,600 cm^{-1}) can also be observed.

STUDIES ON X RAY DIFFRACTOMETRY

Okazaki et al 1982³⁹ studied the effect of fluoride on the physicochemical properties of carbonate-containing apatites, two series of fluoridated CO₃ apatites with various fluoride contents were synthesized at 80°C and pH 7.4. X-ray diffraction was employed to identify precipitates and estimate their lattice constants and crystallinity. Measurements were made on a Rigaku Denki X-ray Diffractometer with graphite-monochromatized CuK α radiation at 35 kV, 23 mA. The x-ray diffraction patterns of all samples were characteristic of calcium apatites. Samples showed a lower degree of crystallization with increase of carbonate content. No extraneous peaks due to CaF₂ were found, indicating that the fluoride content of samples did not exceed 2 mmol/g, which is equal to that of francolite (carbonate fluorapatite). The crystallinity of each fluoridated CO₃Ap initially increased slightly, then decreased with the degree of fluoridation.

Fabbri et al 1995²¹ suggested a method to obtain a substrate of high porosity, exploiting the impregnation of spongy substrate with hydroxyapatite ceramic particles. X-ray diffraction analysis was used to determine newly formed phases. From X-ray diffraction patterns of samples sintered at 1280°C, it is evident that the final product consists of high crystallinity HA, containing less than 4% β -tricalcium phosphate; no other phase is present within the detectable limits. Moreover, all parameters of HA show negligible deviations from those typical (JCPDS no. g-432) of a pure substance.

Best et al 1997²² physically and chemically characterized two synthetic hydroxyapatite powders (A and B), supplied by different manufacturers, in the as-received condition and after heat treatment at 1250°C for 4 h. X-ray diffraction was performed on powder compacts using a Siemens D5000 goniometer, 710 X-ray

generator using CuK α radiation at 30 mA, 40 kV. Scans were performed between 2θ values of 5° and 65° with a step size of 0.03° at two seconds per step. Materials were highly crystalline and exhibited no extraneous phases. However, after heat treatment, while powder A remained phase pure, powder B appeared to contain traces ((5%) of β -TCP.

Peters et al 2000³² did X-ray powder diffraction using a synchrotron source where the photon flux was much higher and the instrumental peak broadening was smaller than with conventional X-ray sources. This was done by a beamline B₂ at HASYLAB/DESY. The samples included callus bone, tumor bone, Endobon and Kiel bone. The samples were measured at room temperature in rotating 1.0-mm glass capillaries in the Debye - Scherrer mode with a wavelength of 120.06 pm. Soller slits were placed between sample and detector. All samples consisted of hydroxyapatite, albeit with different crystallite size as indicated by the peak width. There is no visually detectable difference between the two bone samples and Kiel bone and thus it can be concluded that the mineral phase is unchanged even after the rigorous treatment of Kiel bone. Endobon consists of highly crystalline hydroxyapatite with even higher crystallinity than synthetic hydroxyapatite. It contains a foreign phase that was identified as calcium oxide that remained after decarboxylation of carbonated apatite. The organic matrix did not show up in wide-angle X-ray diffractometry.

Joschek et al 2000²³ studied the properties of a porous hydroxyapatite ceramic produced by sintering of bovine bone were investigated by using a number of physicochemical methods. Porous hydroxyapatite ceramics derived from bovine bone (Endobon) were obtained from Merck, Darmstadt, Germany. Granules from eight different batches with grain sizes between 2.8 and 5.6 mm were used for investigations. After grinding the material in an agate mortar the chemical

composition of the ceramic was investigated by wide Angle X ray Diffractometry. Powder X-ray diffraction spectra were taken using nickel-filtered Cu K α radiation at 40 kV and 20 mA (D5000 diffractometer, Siemens, Munich, Germany). The X-ray diffraction spectrum shows that Endobon is highly crystalline. WAXD data also reveals the presence of CaCO₃, Ca₄O(PO₄)₂ and NaCaPO₄.

Gledhill et al 2001⁴⁰ produced two types of hydroxyapatite coating on titanium substrates by vacuum plasma spraying and detonation gun spraying. These two types of thermally sprayed hydroxyapatite coating with contrasting morphologies were aged under a simulated in vitro environment. The DGUN coatings were sprayed directly onto the grit blasted titanium substrate; the VPS coatings had a thin layer of pure titanium, approximately 20 μ m in thickness, on the surface of the titanium alloy. Groups of coatings were placed in tanks containing Ringer's solution buffered to pH 7.2 and held at 373°C using circulatory heaters. Samples were immersed for periods of one, two, four and eight weeks. After removal from the tanks, coatings were washed in distilled water before being analysed. X-ray diffraction analysis using the Powder Diffraction File PDF-2 database, International Centre for Diffraction Data (ICDD), was used to identify the individual phases present. The region of the X-ray diffraction trace in the range 26- 36° 2 θ was used to determine percentage crystallinity. X ray diffraction showed that there was little change in the composition of the VPS coatings with ageing. A small amount of TCP was detected after eight weeks immersion.

Pilliar et al 2001²⁴ prepared porous structures by gravity sintering calcium polyphosphate (CPP) particles of either 106-150 or 150-250 μ m size to form samples with 30-45 vol% porosity. The X-ray spectrum for the crystallized CPP was produced with a Rigaku diffractometer using a Cu K α radiation source. Diffraction spectra were

compared to published data. X-ray diffraction studies of the sintered samples indicated the formation of β CPP from the starting amorphous powders.

Fulmer et al 2002⁴¹ characterised all materials dried at 250°C for 1 h prior to evaluation. The diffraction peaks of the Norian CRS and BoneSource samples are considerably broader than the Sintered Hydroxyapatite (Calcitite) sample, which is representative of the relative crystallinity of each sample.

Suchanek et al 2002³³ prepared crystalline carbonate- and sodium-and-carbonate-substituted hydroxyapatite (CO_3HAp and NaCO_3HAp) powders at room temperature via a heterogeneous reaction between $\text{Ca}(\text{OH})_2/\text{CaCO}_3/\text{Na}_2\text{CO}_3$ and $(\text{NH}_4)_2\text{HPO}_4$ aqueous solution using the mechanochemical–hydrothermal route. X-ray diffraction (XRD, Kristalloflex D-500, Siemens Analytical X-ray Instrument Inc., Madison, WI) was done using Ni filtered Cu K_α radiation, in the 2θ range of 10–70° at a scan rate of 2.4°/min, with a sampling interval of 0.05°. Crystallographic identification of the as-prepared and heat-treated HAp powders was done by comparing the experimental XRD patterns to standards compiled by the Joint Committee on Powder Diffraction and Standards (JCPDS). Broad XRD peaks can be ascribed to both lattice disorder introduced by the carbonate ions and the very small size of the crystallites. Structural disorder in the as-prepared CO_3HAp and NaCO_3HAp powders has been manifested in the FTIR spectra in the form of broadening of the PO_4 -derived bands. Broadening of XRD peaks was generally more distinct at higher carbonate concentrations.

Porter et al 2003²⁵ studied on the incorporation of silicate into hydroxyapatite which has been shown to significantly increase the rate of bone apposition to HA bioceramic implants. HA and Si-HA filter cakes were processed into granules by

partial grinding and mechanical sieving. After preparation, powders and granules of HA and Si-HA were sintered at 1200°C for 120 min using a ramp rate of 2.5°C/min. The phase composition was assessed by X-ray diffraction using a Phillips D500 diffractometer with CuK_α radiation. Data was collected over the 2θ range 25–40° with a step size of 0.02° and a count time of 2.5 s and was compared with ICDD (JCPDS) standards. The sintered HA, 0.8 and 1.5 wt% Si-HA were phase pure, with no additional phases present.

Tadic and Epple 2004²⁶ studied fourteen different bone substitution materials without any treatment, except for grinding or cutting to a size appropriate for analysis. High-resolution X-ray powder diffractometry (XRD) was carried out in transmission geometry (ground samples on Kapton foil) at beamline B2 at HASYLAB/ DESY, Hamburg, Germany, with wavelengths of about 1.1 Å (A For Ceros, Chronos, Bioresorb, Vitoss and PepGen P-15, diffraction data were measured on a Bruker AXS D8 Advance laboratory instrument (Cu K_α radiation, 1.54 Å). Four of the five β-TCP ceramics show small amounts of impurities besides the major phase. They all exhibit a high crystallinity as indicated by the narrow diffraction peaks. Bioresorb contains some β-Ca₂P₂O₇ (calcium pyrophosphate; peak at 30.8° 2θ) and α-TCP (peak at 22.9° 2θ). Chronos and Ceros contain some α-TCP and some hydroxyapatite (peak at 31.6° 2θ). Vitoss contains some β-Ca₂P₂O₇ (peaks at 29.0 and 30.2° 2θ). In all cases, the amount of foreign phases is very small. Cerabone and Endobon are prepared by high temperature calcination from bovine bone, and consequently the hydroxyapatite is highly crystalline.

Suchanek et al 2004³⁴ prepared magnesium-substituted hydroxyapatite powders with different crystallinity levels at room temperature via a heterogeneous reaction between Mg(OH)₂/Ca(OH)₂ powders and an (NH₄)₂HPO₄ solution using the

mechanochemical-hydrothermal route. X-ray diffraction characterization of all batches of as prepared, purified, and heat-treated Mg-HAp powders was performed using Ni filtered Cu Ka radiation. Samples were analyzed over a 2θ range of $10\text{--}70^\circ$ at a scan rate of $2.4^\circ/\text{min}$, with a sampling interval of 0.05° (XRD, Kristalloflex D-500, Siemens Analytical X-ray Instrument Inc., Madison, WI). Crystallographic identification of the synthesized phases was accomplished by comparing the experimental XRD patterns to standards compiled by the Joint Committee on Powder Diffraction and Standards (JCPDS). With increasing x , the XRD peaks became gradually broader and weaker. This effect could be explained by decreased crystallite size and increased lattice disorder associated with increasing Mg substitution in the HAp lattice.

Susan et al 2005³⁵ prepared nanocarbonated hydroxyapatite/ collagen composite via biomimetic self assembly method. X ray diffraction analysis was performed in a Rigaku/ Multiflex diffractometer with the use of Ni - filtered CuK_α radiation, in the 2θ range of $10^\circ - 80^\circ$ at a scan rate of $2^\circ/\text{min}$, with a sampling interval of 0.02° . The results showed broadening peaks of nanocarbonated hydroxyapatite/ collagen composite are similar to pattern on natural human dentin. Broadening of peaks is distinct at the high collagen sample.

Sena et al 2009²⁸ studied on hydroxyapatite (HA)-type I collagen (Col) composite is a tissue-engineered bone graft which can act as a carrier or a template structure for cells or any other agents. HA/Col composites with HA:Col weight ratios of 80:20; 50:50; 20:80, and 10:90 were produced by the aqueous precipitation method, using a native Type I Col gel. X-ray diffraction (XRD, Rigaku Rota Flex) was used to characterize the crystalline phase. XRD measurements were processed in a powder diffractometer, operating with Cu Ka radiation (1.5418 \AA), 30 kV, 15 mA,

and equipped with graphite monochromator. According to the XRD data refinement results, in the presence of Col, the size of HA crystal suddenly decreased. However, this effect was basically restricted to one single direction.

STUDIES ON DISSOLUTION

Franks et al 2000⁴² studied soluble glasses containing P₂O₅ as a network former and CaO and Na₂O as modifiers. Seven glasses were prepared with the compositions using P₂O₅; NaH₂PO₄; CaHPO₄ and CaCO₃ as starting materials. Two sets of experiments were carried out to determine the solubility. The first experiments were carried out in distilled water. Glass discs were taken and their surface area was measured prior to placing them in glass containers. Distilled water to a volume of 25 ml was added to the containers and these were then incubated at 37°C. At various time points, the samples were removed and excess moisture removed with a tissue and then weighed and was presented as weight loss per unit area. A second set of experiments were carried out under exactly the same conditions except in Hanks Buffered Saline Solution (HBSS) (Gibco BRL, Scotland). All measurements were carried out up to a maximum of 8 weeks. Increasing CaO content in the glasses produces a rapid decrease in solubility. The glasses in distilled water show higher solubility for the same glass measured in HBSS. Glasses with higher CaO content release more Ca²⁺ ions with time into the solution and therefore show a higher decline in the dissolution rate because they can increase the ionic strength. Hence the composition of the glass influences the dissolution rate. High soluble glasses dissolve too quickly to form a layer and high CaO containing glasses do not form this layer at all. The HBSS reduces the solubility and the ion concentration in solution will slow down the diffusion of ions from the glass. Glasses with a CaO content below 16 mol %, the glasses appear

to have a higher solubility in HBSS compared to distilled water. Cl ions in the HBSS strongly react with the Na from the glass, thus significantly increasing the solubility.

Gledhill et al 2001⁴⁰ experimented on two types of thermally sprayed hydroxyapatite coating with contrasting morphologies which were aged under a simulated in vitro environment. Semi-crystalline vacuum plasma sprayed hydroxyapatite coatings and the more amorphous detonation gun sprayed hydroxyapatite coatings were held for various time periods at 37°C in Ringer's solution buffered to pH 7.2. The pH was maintained using hydrochloric acid buffer and tris-hydroxymethylaminomethane. After removal from the tanks, coatings were washed in distilled water before being analysed. It was concluded that the surface roughness of the two types of coating did not appear to change throughout the eight week experimental period. The DGUN coatings were initially rougher than the VPS coatings.

Hankermeyera et al 2002⁴³ conducted a study on The Norian Skeletal Repair Systems (SRS, Norian Corporation, Cupertino, CA), consisting of a calcium phosphate powder and a sodium phosphate solution, as a source of carbonated hydroxyapatite. Hydrochloric acid (HCl) was used as a source of protons for this dissolution study. Atomic absorption analysis (AA) was used in one experiment to quantify directly the dissolution of the CHA powder. A Perkin Elmer Analyst 100 (Perkin Elmer, San Jose, CA) was used at a wavelength of 422.7nm to measure the concentration of calcium dissolved in solution. An increase in [H+] increased the dissolution rate in all the three experimental models. Temperature increase of the acidic solution increased the CHA dissolution rate. The dissolution rate of CHA increased with solution flow rate until the rate became asymptotic. Finally, mechanical agitation of the system via ultrasound acted to increase the CHA

dissolution rate by increasing the rate at which unreacted protons reached the mineral surface, and by mechanically breaking up CHA particles.

Fulmer et al 2002⁴¹ studied the solubility and rate of dissolution of three apatite sources, BoneSource, Norian cranial repair system (CRS), and a sintered hydroxyapatite (Calcitite) in a thermodynamically closed system. Initial dissolution rates at 10 min of BoneSource, CRS, and Calcitite were 0.0465, 0.1589, and essentially 0 mg/min, respectively. Solubility product constants at 37°C were calculated to be 1.49×10^{-35} for CRS, 1.19×10^{-35} for BoneSource, and 2.92×10^{-42} for Calcitite. The increased solubility of the BoneSource and Norian CRS materials over that of Calcitite is related to their poor crystallinity compared to sintered hydroxyapatite. The ground CRS, BoneSource and Calcitite samples of equal mass were placed in separate 250 ml jacketed beakers containing 220 ml 0.03 M tris-buffer (tris(hydroxy)methyl-aminomethane-HCl) at pH=7.3. 50ml of tris-buffer was taken for elemental analysis to be used for calculating the average of four measurements of background calcium concentrations. One 12 ml aliquot of solution was taken at 10, 30, and 60 min, 4, 8, 24, 48, and 120 h. At 120 h and subdivided into three to obtain an average concentration. Spectroscopic elemental analyses were performed with a Spectro EOS combination sequential/simultaneous inductively coupled plasma ICP spectrometer. The Norian CRS and BoneSource materials, which both have carbonate substitutions and reduced crystallinity, had comparable solubilities of 7.4 and 7.5 ppm respectively at pH 7.4 and 37°C. Sintered hydroxyapatite, being highly crystalline with no ionic substitutions, had a much lower solubility of 1.4 ppm. These values are similar to those reported previously for poorly crystalline (9.6 ppm) and sintered (1.4 ppm) hydroxyapatite. Initial dissolution rates calculated for the three apatites at 10

min were 0.159 ± 0.008 mg/min for CRS, 0.0465 ± 0.0023 mg/min for BoneSource, and essentially 0 for Calcitite.

Nilsson et al 2004⁴⁴ investigated a material consisting of calcium sulphate mixed with hydroxyapatite. The material was studied both in vitro in simulated body fluid (SBF) and in vivo when implanted in rat muscles and into the proximal tibiae of rabbits. 12 cylindrical specimens were prepared, 13 mm in diameter and 26 mm in height, six of which contained vitamin E (CS-HA-vitE) and the other six did not (CS-HA). All 12 samples were immersed in 20 ml of SBF at pH 7.4 and 37°C in polyethylene pots with covers. The SBF was changed at four and six days. After seven days in the solution, the samples were removed from the pots and their size measured. The CS-HA-vitE specimens had a lower density than the CS-HA specimens. The results showed slight increase in weight between one and three days in SBF. These increases were 2.0% and 1.7% for CS-HA and CS-HA-vitE, respectively. They continued until day 7. During ten days of immersion in SBF, a small decrease in strength was detected. The dissolution occurred faster in vivo than in vitro.

Li et al 2009⁴⁵ studied the equilibrium solubility of Mg-containing β -tricalcium phosphate (β MgTCP) with various magnesium contents and this was determined by immersing β MgTCP powder for 27 months in a CH_3COOH – CH_3COONa buffer solution at 25 °C under a nitrogen gas atmosphere. The 27-month immersion was performed without shaking in a nitrogen gas atmosphere to avoid contamination with atmospheric CO_2 . The suspensions were then filtered using a Millipore filter of 0.22 μm pore size. The immersion solutions were analyzed for calcium, phosphorus and magnesium using the model SPS 7800 inductively coupled

plasma (ICP) spectrometer (Seiko Instruments, Tokyo, Japan), within an error of $\pm 1.0\%$. It should be noted that the pK_{sp} of β MgTCP after the 27-month immersion were significantly higher than those after the 3-month immersion under air ambient. The equilibrium solubility of β MgTCP decreased with increasing magnesium content of β MgTCP up to 10 mol.%.

Yang et al 2008⁴⁶ measured the dissolution of calcium phosphate filaments made by extrusion freeforming for hard tissue scaffolds. Calcium and phosphate concentrations were measured separately by inductively coupled plasma (ICP) atomic emission spectroscopy. 0.3 g sintered filaments extruded with the 300 μ m die were immersed in 200 ml aqueous 0.03 M tris-buffer solution (tris(hydroxyl)methyl-aminomethane-HCl, ex Sigma) at pH 7.3 and at 37°C to investigate the effects of HA/TCP ratio and sintering temperature on dissolution. The results clearly showed that as the β -TCP content increased, the dissolution increased. Higher sintering temperatures, with consequent closure of surface pores, resulted in lower dissolution.

Esther et al 2012³⁸ used chlorapatite single crystals prepared from the molten salt method with CaCl_2 as a flux. By manipulating the processing conditions (amount of flux, firing time and temperature, and cooling rates) it is possible to manipulate the crystal morphology from microscopic fibres to large crystals. 0.5 g of ClAp crystals were immersed in 50 ml Hanks' solution in polyethylene bottles. The solution was maintained static (without stirring) and the bottles were stored at 37°C for periods ranging from 1 to 32 days. After the each specified time period the samples were removed from the oven, filtered and analysed. Calcium and phosphorus concentrations in solution were measured by ICP and chloride concentration by using a selective electrode (9617BNWP) attached to Thermo Benchtop pH/ISE Model 720A. It was concluded that the presence of defects in single crystals plays an

important role in the dissolution process in acidic conditions. The Cl⁻ concentration keeps increasing up to 16 days. This means that ClAp crystals keep dissolving and CaP precipitating. The initial decrease of chloride concentration in the first 5 days is probably due to salt precipitation.

Materials & Methods

MATERIALS USED

The 5 different alloplastic bone graft materials used for this study are:-

- a) Monophasic Hydroxyapatite – Biograft HA
- b) Tricalcium Phosphate –Biograft TCP
- c) Biphasic Hydroxyapatite which contains Hydroxyapatite and Tri Calcium Phosphate– Biograft HT
- d) Bioactive Glass - PerioGlas
- e) Combination of Hydroxyapatite and Bioactive Glass – Biograft HABG Active

The following data was taken from the manufacturer`s instructions. All samples were obtained in sealed vials as provided by the manufacturer and was used in the present study without any further treatment, except for grinding or cutting to a size appropriate for each analysis.

Biograft HA – porous synthetic hydroxyapatite granules/block. It is biocompatible, non toxic, non inflammatory and bioactive. It causes no immunological, foreign body or irritating response and has an osteoconductive property. The size of the porous granules are 350-500 microns.

Biograft β TCP is porous synthetic β Tri Calcium Phosphate granules/blocks. Biograft β TCP is biocompatible, non toxic, resorbable, non inflammatory and bioactive. It causes no immunological, foreign body or irritating response and has osteoconductive property.

Biograft HT – porous biphasic synthetic hydroxyapatite and β tricalcium phosphate in the ratio of 60:40 and is available as granules/blocks. It is osteoconductive. Biograft HT is biocompatible, non toxic, partially resorbable, non

inflammatory and bioactive. It causes no immunological, foreign body or irritating response and has an osteoconductive ability.

Perioglas is Bioactive Glass. It is manufactured by US biomaterials, Alachua, Florida, USA with a particle size of 90-710microns. Particle shape is irregular. The material is composed of Silicon Dioxide (45%), Calcium Oxide (24.5%), Phosphorus Pentoxide (6%). Bioglass forms direct bond to bone without fibrous tissue in between. This is by formation of carbonated HA over the surfaces of these compounds from natural tissue environment. It is manufactured by a traditional method called melt derived technique.

Biograft HABG Active is a synthetic bioceramic composite intended for surgical implantation. It is supplied in the form of sterile porous granules in the size of 150-700 microns. This ensures effective condensation of the material at the surgical site. The granules are microporous in structure. The glassy part will resorb fast, leaving gaps and pores for new bone to grow. It is a unique bioactive composite which is osteo integrating and resorbable. This material has been developed and patented in India by a dedicated biomaterials research team. It a new generation bone graft substitute which can lead to faster healing of the defect. The material contains hydroxyapatite and calcium - phospho - silicate glass in an optimum ratio. The graft is a mixture of 50% hydroxyapatite and 50% bioactive glass. The glassy part is 17% silicon, 53% calcium and 30% phosphorus. It is made through low temperature sol gel route and composited with hydroxyapatite and tricalcium phosphate phases. It has excellent bone bonding and high resorption compared to conventional hydroxyapatite based implant materials.

All the above mentioned materials were tested for the chemical contents and trace element levels, as per International Standards. It is indicated for repair of periodontal intrabony defects and periapical cysts and for filling extraction sockets. The material satisfies the toxicological safety criteria which have been established through animal studies.

METHODS

MATERIAL CHARACTERIZATION

Once the material is synthesized, it is essential to characterize its property before intended in vivo application. The following tests were done at Sree Chitra Institute of Medical Science and Technology, Poojapura, Thiruvananthapuram.

The physicochemical characterization will be tested under the following headings:-

1. Scanning Electron Microscopy [SEM] – assess the sample`s surface topography, and particle size.
2. Thermogravimetry [TG] - reflect divergent physical properties and chemical compositions among the specimens resulting from their diverse thermal histories.
3. Fourier Transform Infrared Spectroscopy [FTIR] - to provide information concerning the chemical composition and the major functional groups.
4. X ray diffractometry [XRD] - used to identify phase and composition features and qualitatively evaluate the crystallinity of the materials
5. Dissolution rates - to find the solubility rate of calcium and silica from the materials tested.

SCANNING ELECTRON MICROSCOPY

A scanning electron microscope (SEM) is a type of electron microscope that images a sample by scanning it with a beam of electrons in a faster scan pattern. The electrons interact with the atoms that make up the sample producing signals that contain information about the sample's surface topography, composition, and other properties such as electrical conductivity. The types of signals produced by a SEM include secondary electrons, back-scattered electrons (BSE), characteristic X-rays, light (cathodoluminescence), specimen current and transmitted electrons. The signals result from interactions of the electron beam with atoms at or near the surface of the sample. In the most common or standard detection mode, secondary electron imaging or SEI, the SEM can produce very high-resolution images of a sample surface, revealing details less than 1 nm in size. Due to the very narrow electron beam, SEM micrographs have a large depth of field yielding a characteristic three-dimensional appearance useful for understanding the surface structure of a sample.

For conventional imaging in the SEM, specimens must be electrically conductive, at least at the surface, and electrically grounded to prevent the accumulation of electrostatic charge at the surface. Metal objects require little special preparation for SEM except for cleaning and mounting on a specimen stub. Nonconductive specimens tend to charge when scanned by the electron beam, and especially in secondary electron imaging mode, this causes scanning faults and other image artifacts. They are therefore usually coated with an ultrathin coating of electrically conducting material, deposited on the sample either by low-vacuum sputter coating or by high-vacuum evaporation. Conductive materials in current use for specimen coating include gold, gold/palladium alloy, platinum, osmium, iridium, tungsten, chromium, and graphite.⁴⁷

In the present study, granules were washed with acetone and deionised distilled water, air dried and critically point dried to remove moisture. Then topography of the samples were viewed with SEM (FEI QUANTA 200 Environmental Scanning Electron Microscope (Refer color plates 1a and 1b). Here, the samples were used in the as received condition due to use by a low vacuum machine.

THERMOGRAVIMETRY

Thermogravimetric analysis uses heat to drive reactions and physical changes in materials. TGA provides a quantitative measurement of any mass change in the polymer or material associated with a transition or thermal degradation. TGA can directly record the change in mass due to dehydration, decomposition or oxidation of a polymer with time and temperature. Thermogravimetric curves are characteristic for a given polymer or compound because of the unique sequence of the physicochemical reaction that occurs specific temperature ranges and heating rates and a function of the molecular structure. The changes in mass are a result of the rupture and /or formation of various chemical and physical bonds at elevated temperatures that lead to the evolution of volatile products of the formation of heavier reaction products.

TGA is a technique in which the mass of a substance is measured as a function of time or temperature while the substance is subjected to a controlled temperature program.⁵⁵ The gaseous environment of the sample can be: ambient air, vacuum, inert gas, oxidizing/ reducing gases, corrosive gases, carburizing gases, vapors of liquids or self generating atmosphere. The pressure can range from high vacuum or controlled vacuum, through ambient, to elevated and high pressure; the latter is hardly practical due to strong disturbances. By measuring the temperature at which such reactions

occur and the heat involved in the reaction, the compound present in the material can be categorized. The physical and chemical changes that take place when an unknown sample is heated provide information that enables to identify the material. These changes also indicate the temperature at which the material ceases to be stable under conditions. From room temperature to about 200°C, incorporated water is lost. Above about 300°C, organic material like collagen, fat tissue, proteins start to burn. At about 400°C, only the mineral phase (calcium phosphate) is left. If the mineral contains some carbonate in the form of carbonated apatite, there is a mass loss between about 400°C and 900°C.

The equipment consists of a furnace for measuring the temperature of the sample, a balance for continuously weighing the sample. The sample was loaded into the crucible and a counterweight added to restore the arms of the balance to equilibrium. The furnace was heated at a controlled rate, starting from the lowest temperature and ending at temperatures as high as 1000°C. The rate at which the temperature was increased was slow enough to allow the sample to remain close to chemical and thermal equilibrium with its surroundings throughout the heat treatment. If the sample was heated too rapidly, the apparent temperatures at which chemical or physical changes took place would appear to be too high. If the rate at which the sample was heated were too slow, the experiment would take too long.⁴⁸

In the present study, thermogravimetry was conducted using SDTQ 600 (Refer color plate 2, 3, 4 and 5). Platinum or alumina pans were used for weighing the samples. The pans were first kept empty and weighed before placement of the samples. This acted as a control. A sample of material was placed on an arm of recording microbalance, also called thermobalance and that arm and the sample were placed in a furnace. The gaseous environment of the sample is 99.99% pure Nitrogen

with moisture 1ppm and Oxygen 1ppm. The purge rate was 100+/- 5ml/min and the pre purge time is 5minutes. The furnace temperature is controlled in a pre – programmed temperature/ time profile or in the rate – controlled mode, where the pre programmed value of the weight changes imposes the temperature change in the way necessary to achieve and maintain the desired weight – change rate. The change in sample weight is recorded while the sample is either maintained isothermally at a temperature of interest or subjected to a programmed heating. Here, the temperature was increased from room temperature upto 1000°C at a heating rate of 20°C/minute.

FTIR - FOURIER TRANSFORM INFRARED SPECTROSCOPY

IR was discovered in 1800 by Sir William Herschel. IR absorption investigation of materials began in 1900. First commercial IR spectroscopy was available at the end of World War II. Studies of polymers were among the first applications of the method. IR spectroscopy is probably the method most extensively used for investigation of polymer structure and analysis of functional groups. IR spectroscopy was used to study samples in gaseous, liquid and solid state, depending on types of accessories used. IR has been used to characterize polymer blends, dynamics, surfaces and degradation products. It is capable of qualitative identification of the structure of unknown materials as well as quantitative measurement of the components in a complex mixture.

Covalently bonded atoms forming an organic molecule do not maintain fixed positions relative to one another but vibrate about an average interatomic distance. Absorption of electromagnetic radiation of the appropriate energy excites the atoms. The absorbed energy is then converted to vibrational and rotational motion. The resulting increase in molecular vibrations leads to changes of interatomic distances

and angles of the molecules. The frequency of electromagnetic radiation within the infrared region giving rise to the absorption process depends on the relative masses of the atoms, force constants of the bonds and geometry of the atoms comprising the molecule. It is assumed that the molecular vibrations move atoms toward and away from each other in simple harmonic motion.⁴⁸

In this study, the pelleted sample was analysed using FTIR spectrophotometer (Thermo Electron Corporation – (Refer color plate 6 and 7). The samples are first ground using an agate mortar and pestle (Refer color plate 8). If it is a liquid sample, it is coated with KBr before analyses. The sample is mixed for 5 minutes in a ratio of 1:150 with KBr (Refer color plate 9) and ground into a uniform mixture. KBr or NaCl can be used for preparing the pellet. NaCl is more water absorbing and so it is not frequently used for mixing along with the samples. KBr alone is ground and made into a pellet and is used as a control. The pellet is prepared by placing the mixture into a die (Refer color plate 10) and about 7 tonnes pressure is used for compression (Refer color plate 11 and 12). Compression is done with a Hydraulic Pellet Press (Refer color plate 13 and 14). KBr is added along with the sample and made into a pellet (Refer color plate 15) and is analyzed by placing it into the IR machine (Refer color plate 16 and 17). A graph is obtained using computer programming (Refer color plate 18). The graph which is obtained from the control is subtracted from the graph obtained for each sample. Organic groups like CH,OH gives more reflection in Infrared Spectroscopy. These groups are seen in atmosphere and so the control sample is tested.

X RAY DIFFRACTION (XRD)

X ray diffraction measured the average spacing between layers or rows of atoms. It is used to determine the orientation of a single crystal or grain. Thus it can be used to find the crystal structure of an unknown material. XRD also helps to measure the size, shape and internal stress of small crystalline region. Applications are to determine structural properties like lattice parameters, strain, grain size, epitaxy, phase composition, preferred orientation and thermal expansion. The atomic arrangement could also be assessed by this technique. The method is based on the model by Bragg, and according to this model the crystal structure consists of planes that reflect X-rays. The wavelength of the X-ray is of the same order of magnitude as the bond distances between the atoms in the crystal and therefore produces a pattern unique for the atomic arrangement in the sample. The results obtained for each material was compared with the standards compiled by the Joint Committee on Powder Diffraction and Standards (JCPDS). It was done to characterize the phase purity and crystallinity of the materials. It is a fingerprint of a certain material.⁴⁹

In this study, the test material was placed in an X ray diffractometer (Advance Bruker) (Refer color plate 19 and 20) and the graph obtained was compared to JCPDS. Also, Scherrer equation was used to find the crystal size as follows:-

$$\beta_{1/2} = (K\lambda 57.3)/(D \cos \theta)$$

Here, $\beta_{1/2}$ is the peak width (as full-width at half maximum) in $^{\circ}2\theta$; K is a constant that we set to 1 (as often done), λ is the X-ray wavelength in A, D is the average domain size (roughly the crystallite size) and θ is the diffraction angle of the corresponding reflex.

DISSOLUTION

In this study, first all the beakers and test tubes were thoroughly washed with soap water and then rinsed in running water, following which the equipments were washed with dilute Nitric Acid and again rinsed in running water and then using distilled water and again rinsed with deionised water. Deionised water was made in a deionising unit (Syngery UV Millipore - Refer color plate 21). Then all the equipments were kept for drying. After that, Tris (Pure Analytical Reagent – Assay 99) was prepared.

0.03 M Tris was prepared.

Weight = Concentration x Mass (M) x Volume (Litre)

$$= 0.03 \times 121.14 \times 2(l)2g$$

$$= 7.2684$$

$$\text{pH} = 7.3$$

Tris buffer – Hydroxy Ethyl Amino Methane (SRL – Sisco Research Lab – Refer color plate 22) was prepared. pH was checked and maintained using pH meter [Accumet Model 50 – (Refer color plate 23)]. Tris was prepared using a magnetic stirrer with hot plate [IKA – WERKE – (Refer color plate 24)]. 0.03M Tris buffer was prepared in water at pH 7.3 and temperature of 37°C (Refer color plate 25). The test materials were ground into fine powder using a agate mortar and pestle (Refer color plate 26). 150ml of Tris was mixed with 1 g powder and maintained at 37°C. 250ml jacketed beakers with 220ml 0.03M tris at pH 7.3 was evaluated in a thermodynamically closed system. The measurements were made in a thermodynamically closed system: a given quantity of a solid apatite was placed in a

beaker of the buffer solution and the liquid is stirred. No mass crossed the boundary of the solution. 1 ml dilute (20%) Nitric Acid was combined with 9 ml extract of the aliquot to make it a 10 ml aliquot and aliquots were withdrawn and analyzed quantitatively for the measurement of the calcium concentration [Ca^{2+}]. Aliquots were taken at 10, 30 and 60 minutes, 4, 8, 24, 48 and 120 hours and it was filtered. Then a pipette was used to take the liquid and this was taken in the screw capped tubes. Immediately after taking each aliquot, it was filtered through Millipore Millex-VV sterile filters with 0.22 μm hydrophilic PVDF mesh to remove solids from the liquid. Spectroscopic elemental analyses were performed with a Spectro EOS combination sequential/simultaneous inductively coupled plasma ICP spectrometer (Perkin Elmer Optical Emission Spectrometer Optima 5300 DV – Refer color plate 27).



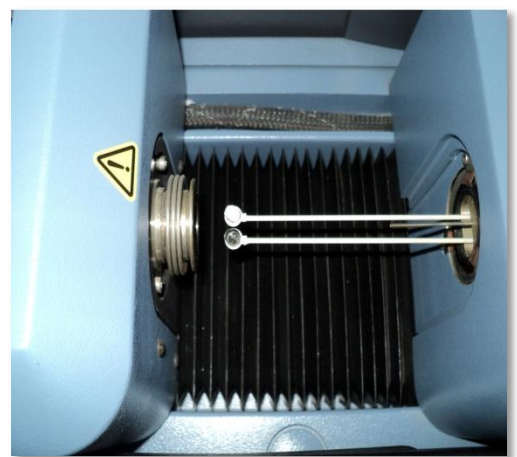
CP 1a: ESEM – Environmental Scanning Electron Microscopy



CP 1b: SEM connected to computer



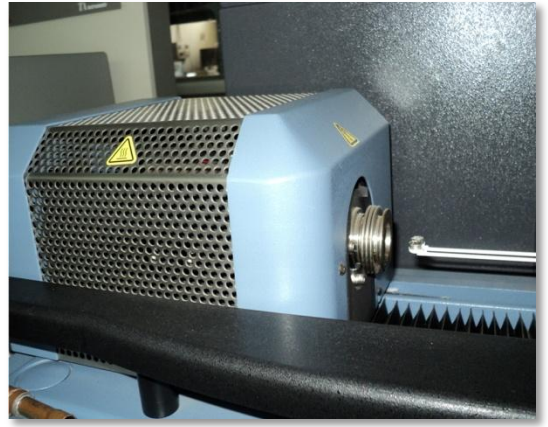
CP2: Thermogravimetry machine closed position



CP3: Alumina crucibles



CP4: Thermogravimetry machine in open position



CP5: Crucible loaded



CP6: FTIR machine in open position



CP7: FTIR machine in closed position



CP8: Agate mortar and pestle



CP9: Test material placed In a die



CP10: Die in closed position



CP11: Die placed in pellet press



CP12: Pressure raised to 1000psi



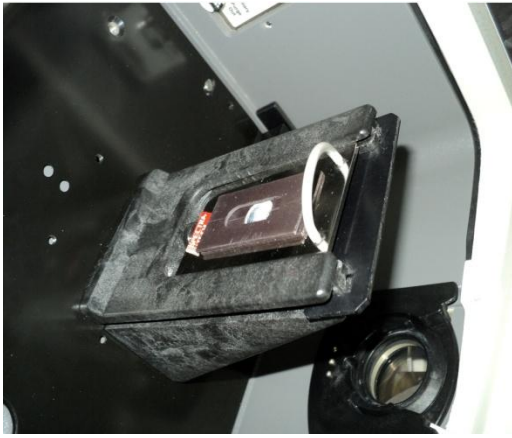
CP13: Hydraulic pellet press by PCI services



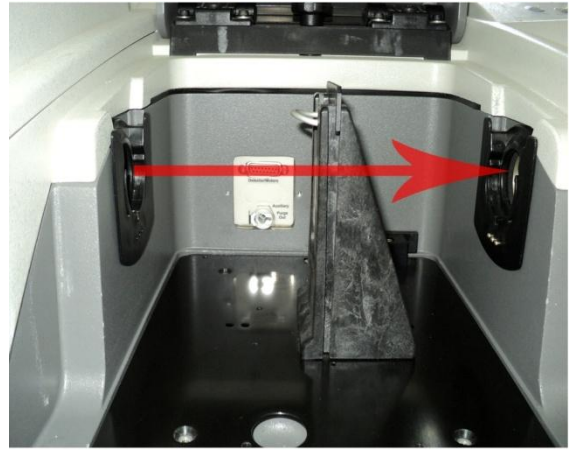
CP14: Hydraulic pellet press by Perkin Elmer



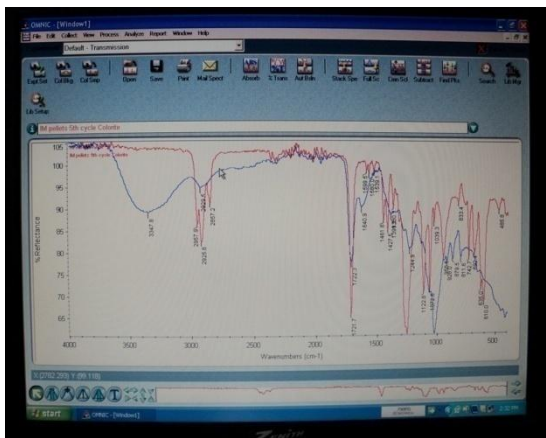
CP15: Pellet obtained



CP16: Pellet placed in FTIR machine



CP17: Passage of infra red rays



CP18: Results seen as graph in computer



CP19: XRD machine



CP20: XRD machine – close up view



CP21: Machine for deionised water preparation



CP22: Prepared TrisHCl
buffer



CP23: pH meter



CP24: Magnetic stirrer



CP25: Thermal vacuum machine



CP26: Agate mortar and
pestle for grinding



CP27: ICP machine

Results and Observations

1. SCANNING ELECTRON MICROSCOPIC ANALYSIS

The 5 alloplastic graft materials were studied for their morphological characteristics using SEM (FEI QUANTA 200 Environmental Scanning Electron Microscope - Germany). The samples were examined as such at low vacuum mode without any coating. The following results were obtained.

1. MONOPHASIC HYDROXY APAPTITE – Biograft HA

In the present study, SEM data shows grains of different sizes as seen under low magnification of 100x for HA. Each particle has a size of approximately 100- 300 microns. Under high magnification of 6000x, definite pores are visible. The pores are micro and nano sized and the particles are composed of nano sized crystallites and appears roughened. The pores have an approximate size of 1 μ m.

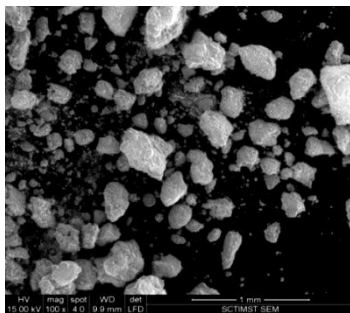


Image A

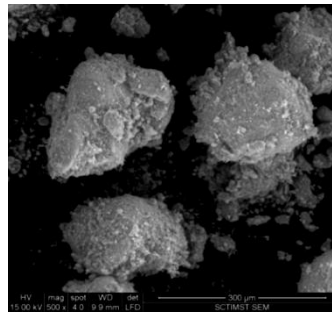


Image B

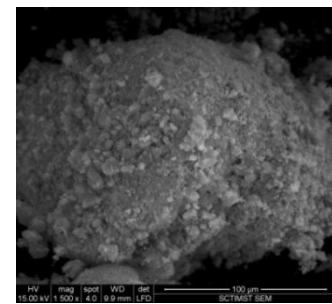


Image C

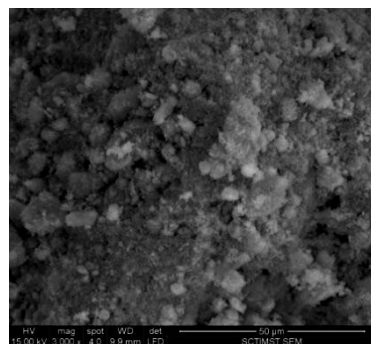


Image D

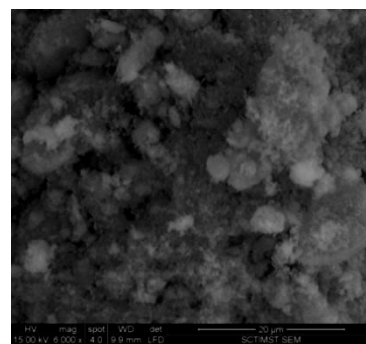


Image E

SEM images of Monophasic Hydroxyl Apatite - Biograft HA: Image A – 100X; Image B – 500X; Image C – 1500X; Image D – 3000X; Image E – 6000X

2. TRICALCIUM PHOSPHATE – Biograft TCP

SEM results show that particles are of different sizes and under low magnification of 100x for TCP. The particle size is approximately 200-300 microns. Under high magnification of 6000x, pore size is approximately 0.5 - 1 μm and the surface of the particle is roughened and is sintered in nature. It can be said that the pores are nano sized and the particles have a needle like structure.

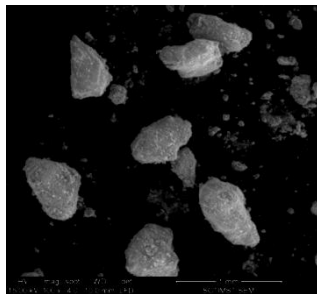


Image A

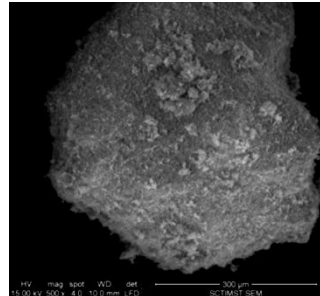


Image B

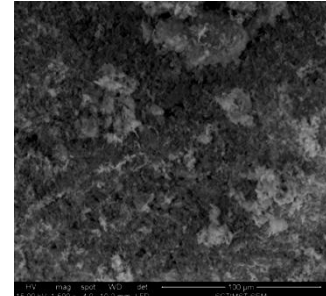


Image C

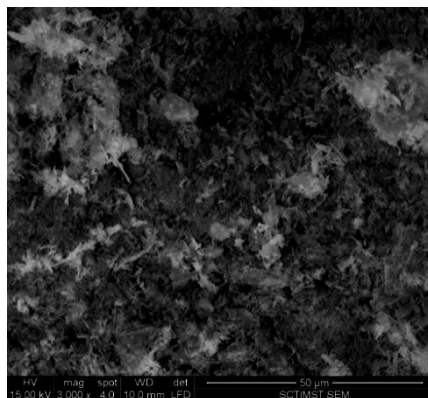


Image D

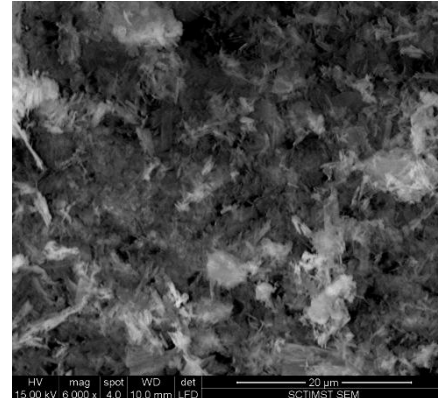


Image E

SEM images of Tricalcium phosphate – Biograft TCP : Image A – 100X; Image B – 500X; Image C – 1500X; Image D – 3000X; Image E – 6000X

3. BIPHASIC HYDROXYAPATITE – Biograft HT

SEM data shows that particles are of almost same size under low magnification of 100x for HT. The grains have a definite shape with smooth edges. The particle size is approximately 0.3- 0.5mm. Under high magnification of 6000x, nano pores are visible and the surface of the particle is almost smooth and is sintered in nature.

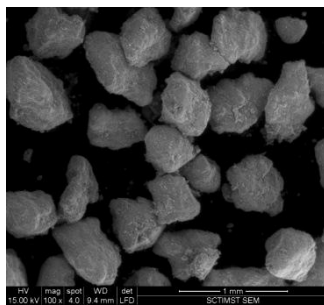


Image A

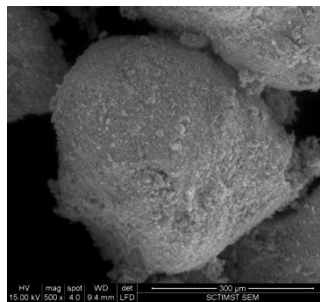


Image B

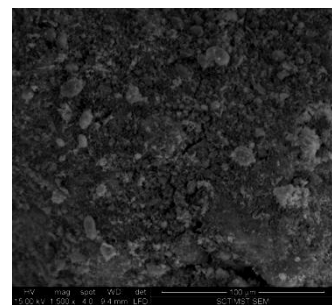


Image C

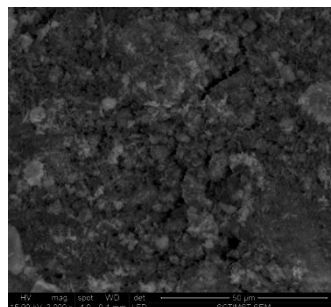


Image D

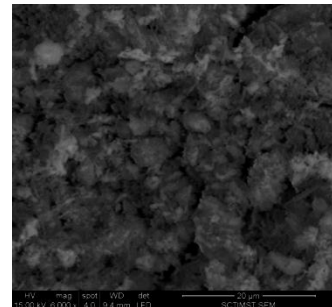


Image E

SEM images Of Biphasic Hydroxyapatite – Biograft HT : Image A – 100X; Image B – 500X; Image C – 1500X; Image D – 3000X; Image E – 6000X

4. BIOACTIVE GLASS - PERIOGLAS

SEM data shows that particles have a definite crystalline shape and size under low magnification of 100x for PG. The particle size ranges between 100-200 microns and has a smooth surface. Under high magnification of 6000x, pores are not visible and surface of the particles are smooth with less roughness. The sharp surfaces of the particles may be due to the presence of glass particles in it. Generally, there is presence of glass particles and there is no crystallinity of the sample at high magnification.

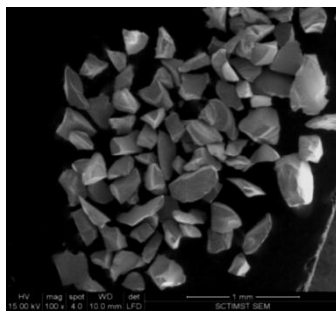


Image A

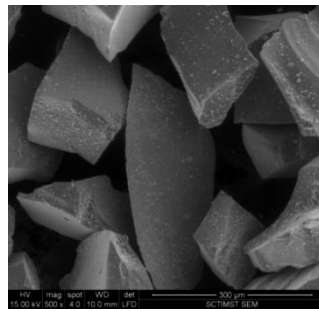


Image B

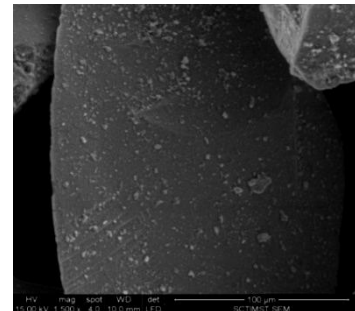


Image C

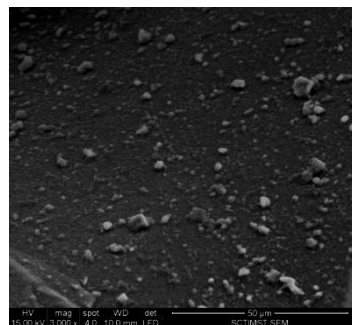


Image D

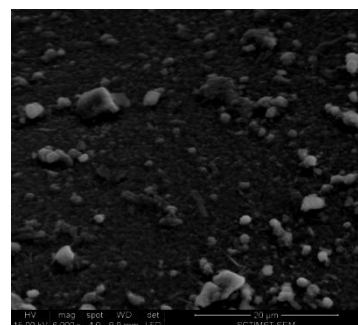
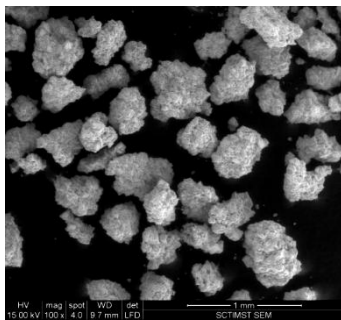
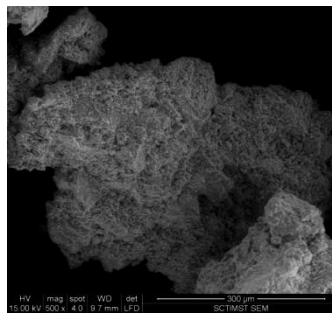
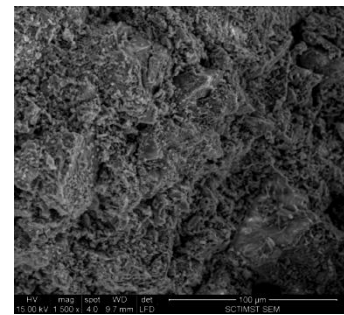
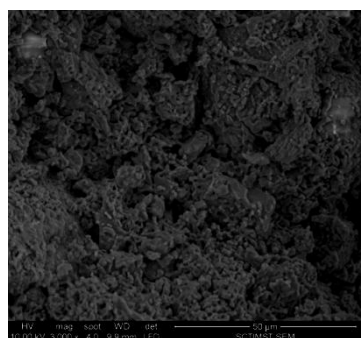
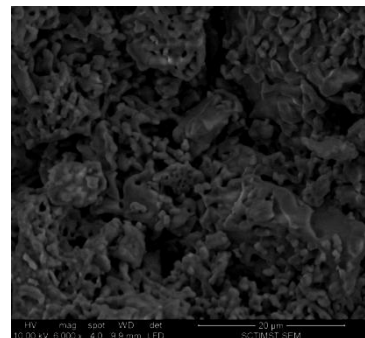


Image E

SEM images of Bioactive Glass – PerioGlas : Image A – 100X; Image B – 500X; Image C – 1500X; Image D – 3000X; Image E – 6000X

5. HYDROXYAPATITE BIOACTIVE GLASS COMBINATION -Biograft HABG Active

SEM data of HABG shows that grains are of different sizes under low magnification of 100x for HABG. The particles are seen as regular sized agglomerates. The particle size is approximately 500 – 700 microns. Under high magnification of 6000x, The material is highly porous with fine pores. Particles are needle shaped and pores are irregular with an approximate size of 0.5 - 1 microns. The particle size is submicron in nature. The high magnification picture shows a partially melted appearance due to the presence of glass.

**Image A****Image B****Image C****Image D****Image E**

SEM images of Hydroxyapatite Bioactive Glass Combination -Biograft Habg Active : Image A – 100X; Image B – 500X; Image C – 1500X; Image D – 3000X; Image E – 6000X

Table 1 - Particle size by SEM – at low magnification of 100x

Material tested	Size of the particle (nm)
HA	100-300
TCP	200-500
HT	300-500
PG	100-200
HABG	250-500

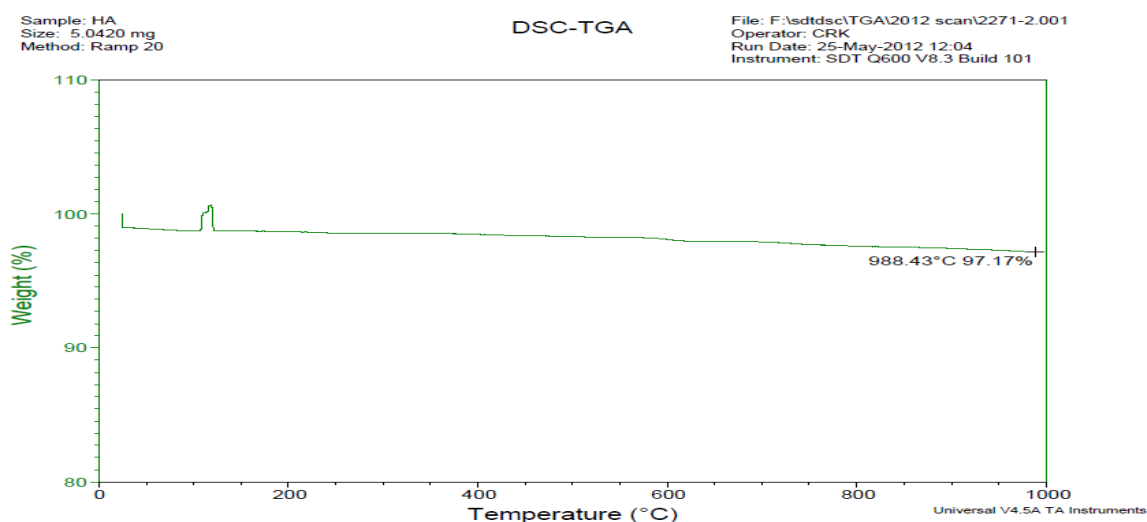
Table 2 - Pore size by SEM – at high magnification of 6000x

Material tested	Size of the pore (nm)
HA	0.1
TCP	0.5-1
HT	Nano pores
PG	Dense
HABG	0.5-1

2. THERMOGRAVIMETRIC ANALYSIS

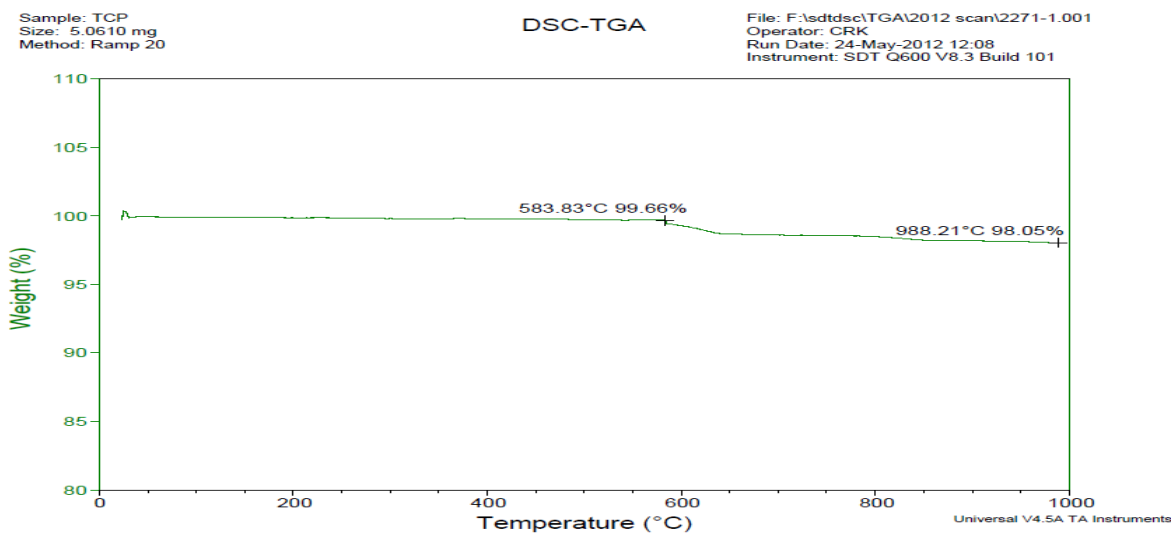
Thermogravimetric analysis or thermal gravimetric analysis (TGA) is a method of thermal analysis in which changes in physical and chemical properties of materials are measured as a function of increasing temperature (with constant heating rate), or as a function of time (with constant temperature and/or constant mass loss). In this study, thermogravimetric analysis was conducted using SDTQ 600. Thermogravimetric analysis was done to assess mineral and carbonate content.

1. MONOPHASIC HYDROXY APAPTITE – Biograft HA



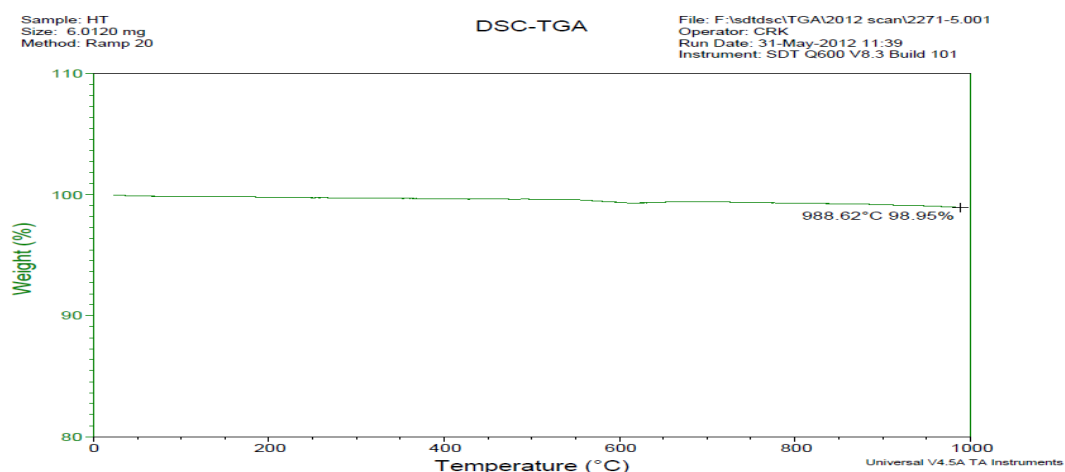
For HA – At 988.43°C, weight was 4.899mg and weight% was 97.17%. TGA shows that HA does not contain adsorbed water/ lattice water or any organic phases present in it. So there is weight loss of 2.83%.

2. TRICALCIUM PHOSPHATE – Biograft TCP



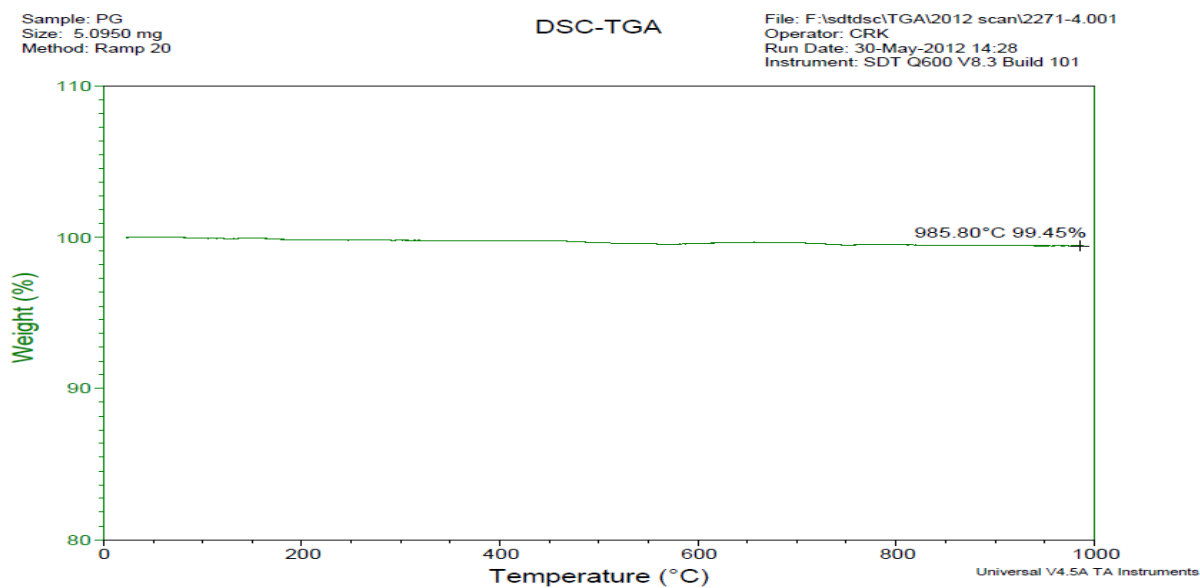
TGA shows that TCP does not contain adsorbed water/ lattice water or any organic phases present in it. So there is weight loss of 1.95%. For TCP - at 583.83°C, weight was 5.044mg and weight% was 99.66%. At 988.21°C, weight was 4.962mg and weight % was 98.05%

3. BIPHASIC HYDROXYAPATITE – Biograft HT



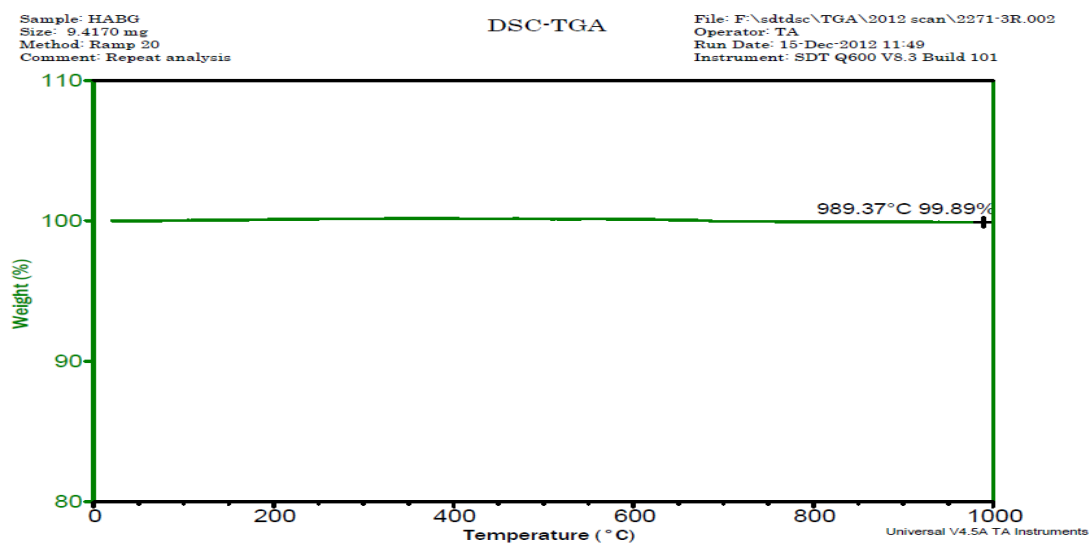
For HT, TGA results show that at 988.62°C, weight loss was 5.949mg and weight% was 98.95% after heating to 1000°C.

4. BIOACTIVE GLASS - PERIOGLAS

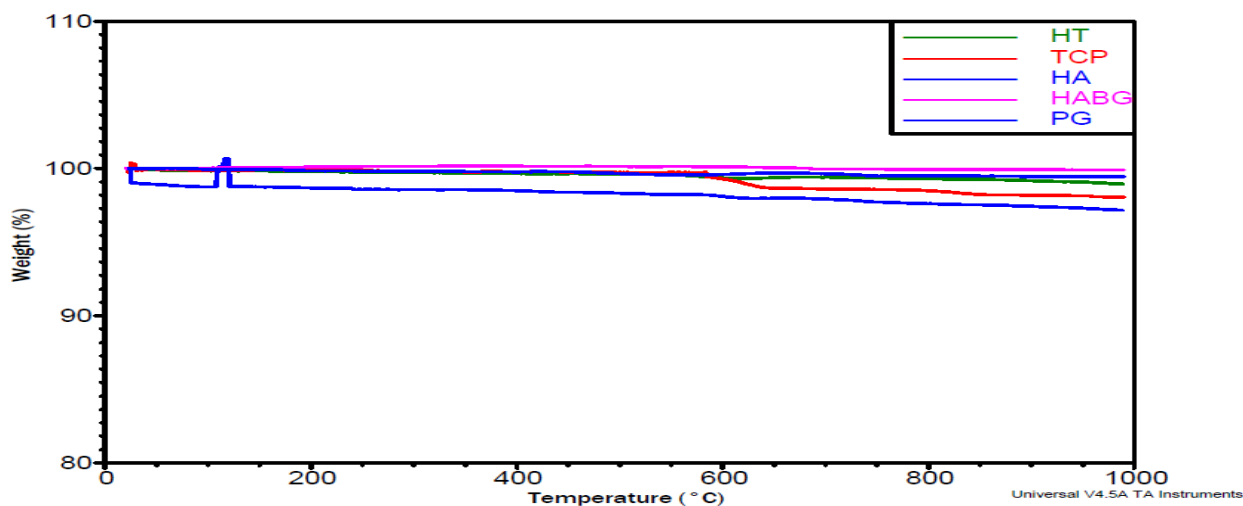


TGA shows that PG does not contain adsorbed water/ lattice water or any organic phases present in it. A weight loss of 0.55% is seen when heated upto 1000°C. Remaining weight is 99.45%.

5. HYDROXYAPATITE BIOACTIVE GLASS COMBINATION - Biograft HABG



For HABG- At 666.88°C, weight was 6.136mg and weight% was 100.9%. TGA shows that HABG does not contain adsorbed water/ lattice water or any organic phases present in it. So there is weight loss of 0.11%.



Stacked TGA results of 5 samples

For TCP - at 583.83°C, weight was 5.044mg and weight% was 99.66%

At 988.21°C, weight was 4.962mg and weight % was 98.05%

For HA – At 988.43°C, weight was 4.899mg and weight% was 97.17%

For HABG- At 666.88°C, weight was 6.136mg and weight% was 100.9%

For PG – At 985.80%, weight was 5.067mg and weight% was 99.45%

For HT – At 988.62°C, weight was 5.949mg and weight% was 98.95%

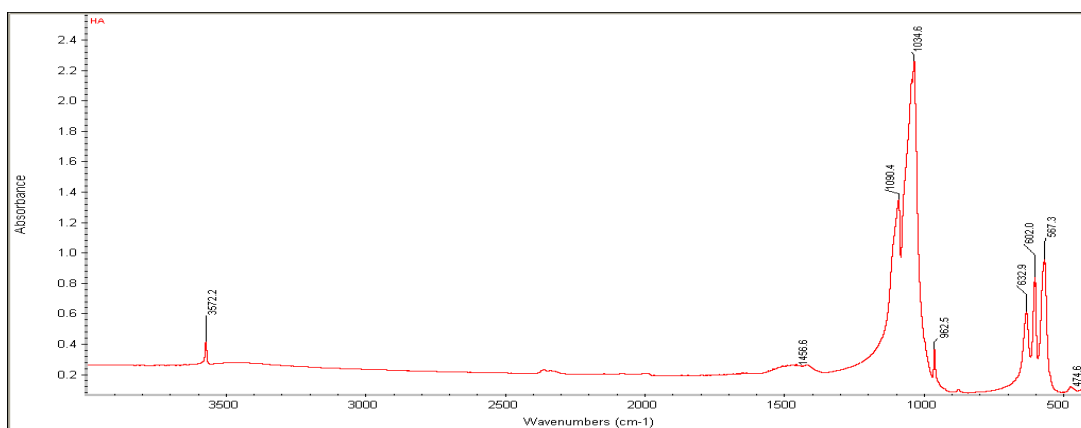
The stacked result shows that all the test samples show a minimal weight loss only upto 2%. This can be attributed to the moisture content present or due to oxidation of the samples. From TGA data, it can be concluded that there is no adsorbed water/lattice water in any of the tested samples. Also, there is absence of any organic part as samples were already sintered by the manufacturer. This is because all the test

materials used were synthetic/alloplastic graft materials. The results of thermogravimetry show that all the tested materials are stable upto 1000°C. Thus, all test materials are thermally stable, pure and contain no impurities.

3. INFRA RED SPECTROSCOPIC ANALYSIS

Infrared spectroscopy (IR spectroscopy) is the spectroscopy that deals with the infrared region of the electromagnetic spectrum, that is light with a longer wavelength and lower frequency than visible light. It covers a range of techniques, mostly based on absorption spectroscopy. As with all spectroscopic techniques, it can be used to identify and study chemicals. A common laboratory instrument that uses this technique is a Fourier transform infrared (FTIR) spectrometer. In this study, the pelleted samples were analysed using FTIR spectrophotometer (Thermo Electron Corporation).

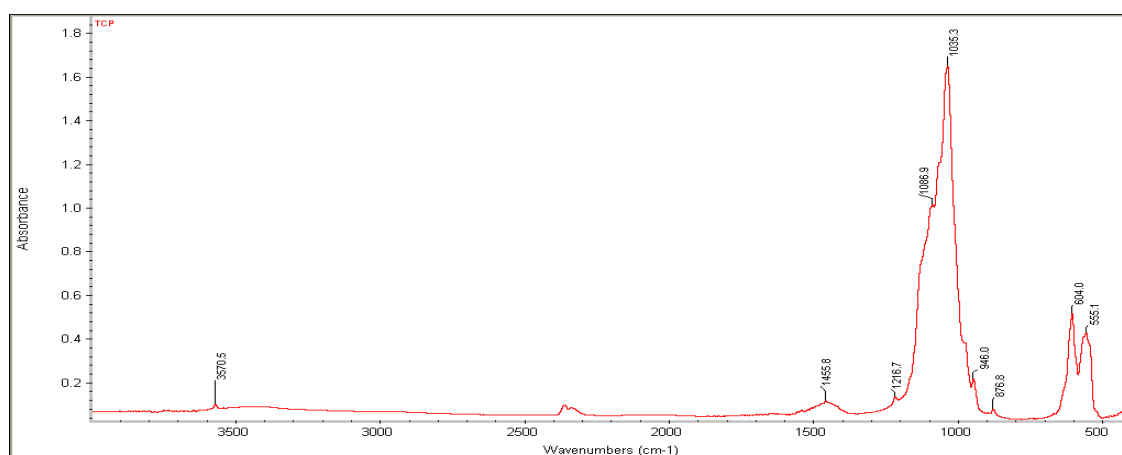
1. MONOPHASIC HYDROXY APAPTITE – Biograft HA



FTIR pattern of HA shows 2 clusters of peaks between 1200 and 900 cm^{-1} and also between 650 and 400 cm^{-1} . The peak between 1200 and 900 cm^{-1} shows PO_4 stretching and that between 650 and 400 cm^{-1} indicates PO_4 bending. Vibrational

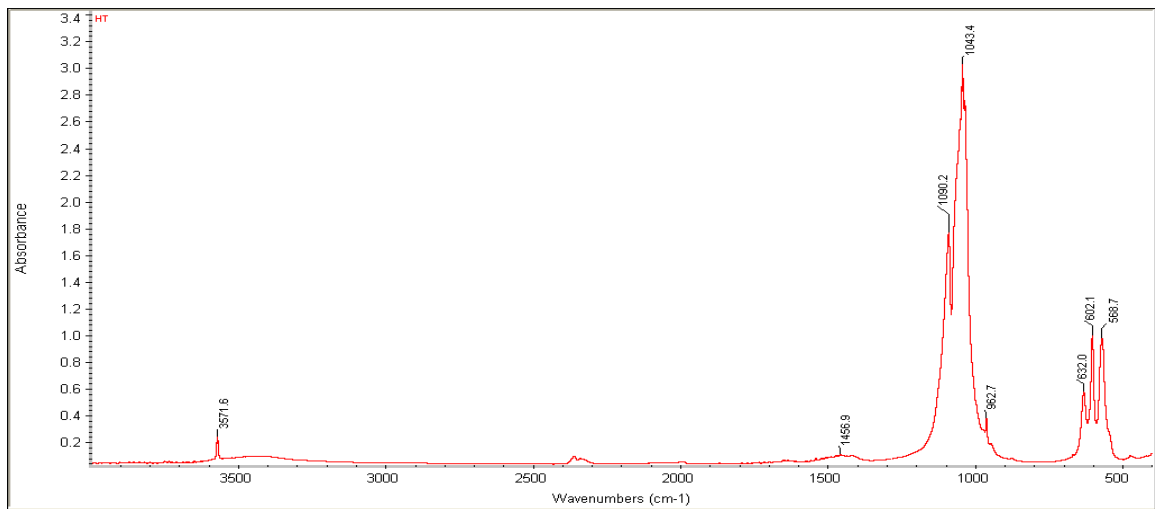
peaks ν_1 is seen at around 960 cm^{-1} . ν_3 is seen at 1090 and 1045 cm^{-1} . ν_1 and ν_3 shows PO_4 stretching. ν_4 is a vibrational peak at about $600\text{-}570\text{ cm}^{-1}$. There is also presence of a weak band at about 470 cm^{-1} which indicates ν_2 . ν_2 and ν_4 indicates vibration phases. 3570 cm^{-1} and 630 cm^{-1} shows OH stretching and vibration. The peaks at 1450 cm^{-1} , 1420 cm^{-1} and 870 cm^{-1} shows CO_3 group.

2. TRICALCIUM PHOSPHATE – Biograft TCP



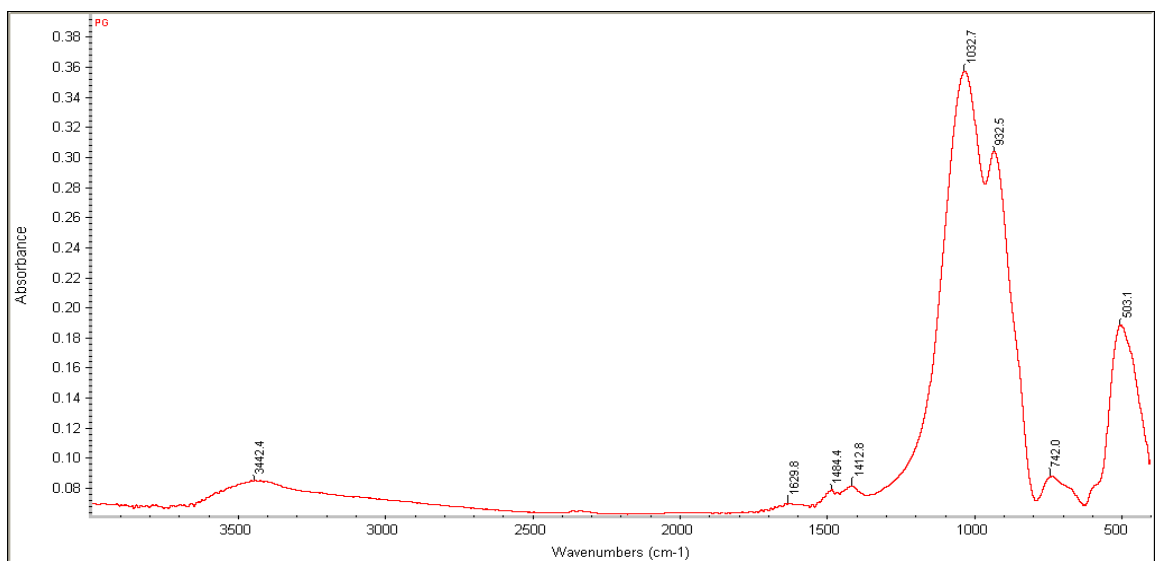
TCP shows PO_4 stretching at 1035.3 cm^{-1} . FTIR pattern of TCP shows 2 clusters of peaks between 1200 and 900 cm^{-1} and also between 650 and 400 cm^{-1} . The peak between 1200 and 900 cm^{-1} shows PO_4 stretching and that between 650 and 400 cm^{-1} indicates PO_4 bending. Vibrational peaks ν_1 is seen at around 960 cm^{-1} . ν_3 is seen at 1090 and 1045 cm^{-1} . ν_1 and ν_3 shows PO_4 stretching. ν_4 is a vibrational peak at about $600\text{-}570\text{ cm}^{-1}$. There is also presence of a weak band at about 470 cm^{-1} which indicates ν_2 . ν_2 and ν_4 indicates vibration phases. 3570 cm^{-1} shows OH stretching. Peaks at 1450 cm^{-1} , 1420 cm^{-1} and 870 cm^{-1} shows CO_3 group.

3. BIPHASIC HYDROXYAPATITE – Biograft HT



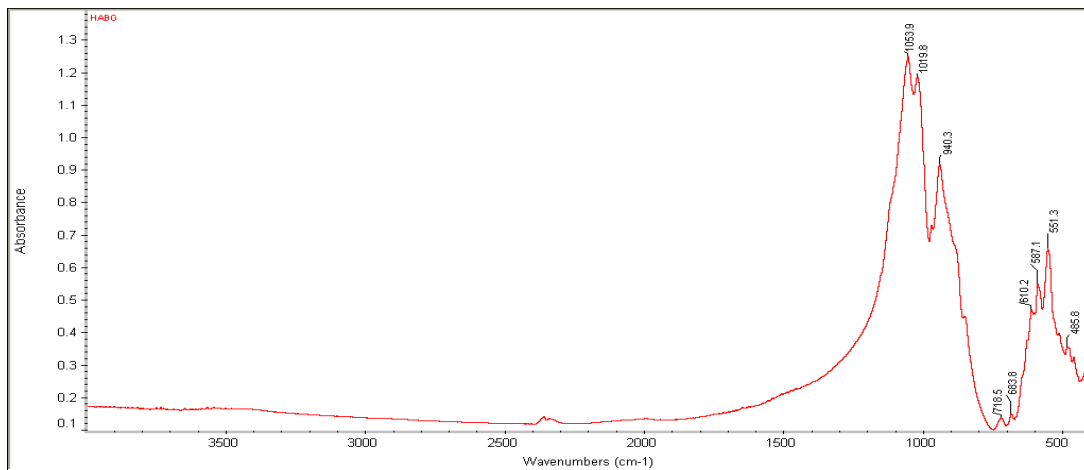
In HT, OH peak is seen at 3571.6 cm^{-1} and it is sharp. There is presence of PO_4 stretching at 1034 cm^{-1} . FTIR data shows 2 clusters of peaks between 1200 and 900 cm^{-1} and also between 650 and 400 cm^{-1} . The peak between 1200 and 900 cm^{-1} shows PO_4 stretching and that between 650 and 400 cm^{-1} indicates PO_4 bending. There is also presence of a weak band at about 470 cm^{-1} which indicates ν_2 .

4. BIOACTIVE GLASS - PERIOGLAS

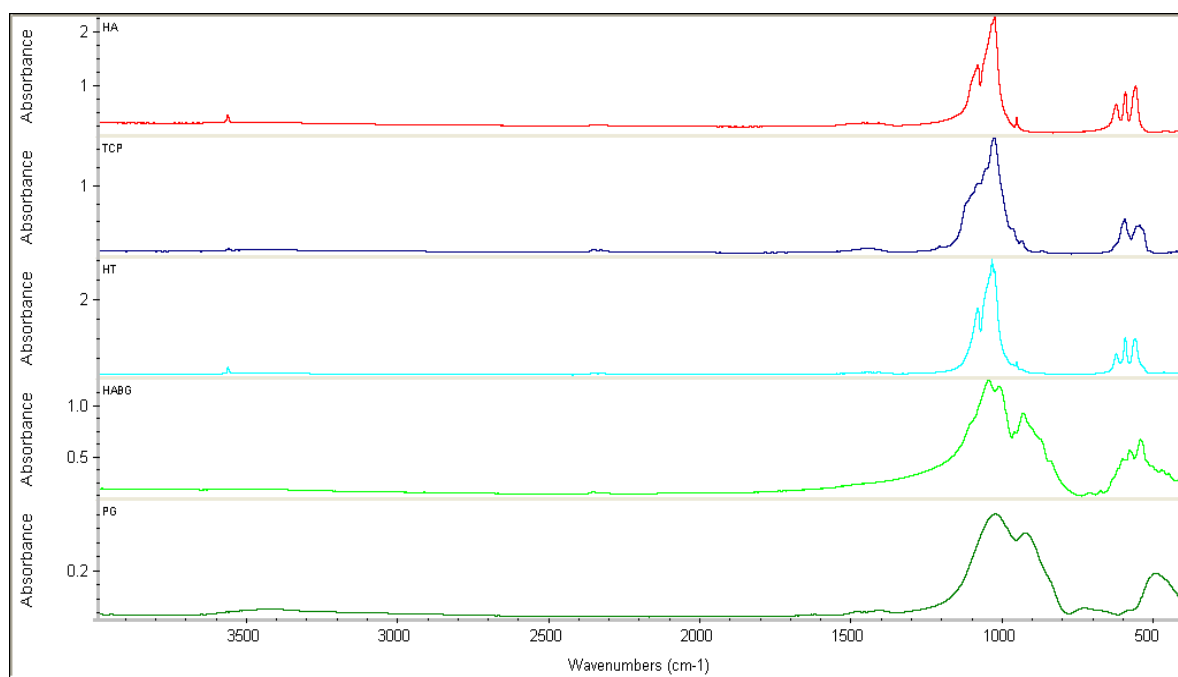


Perioglas shows moisture content as a peak seen at 3442.4cm^{-1} . PO_4 stretching is seen at 1032.7cm^{-1} and it is extended and broadened. Silica is seen at 503.1 cm^{-1} . The PO_4 peak is broad due to the amorphous nature which is also evident in infra red spectroscopy results. The broad PO_4 peak may be due to the amorphous nature of the material.

5. HYDROXYAPATITE BIOACTIVE GLASS COMBINATION -Biograft HABG Active



FTIR pattern of HABG, OH peak is absent. OH peak is masked by the presence of silica in HABG. Silica peak is seen at 551.3cm^{-1} . 2 clusters of peaks are seen between 1200 and 900 cm^{-1} and also between 650 and 400 cm^{-1} . The peak between 1200 and 900 cm^{-1} shows PO_4 stretching and that between 650 and 400 cm^{-1} indicates PO_4 bending.



Stacked Infra Red Spectroscopic results for 5 samples

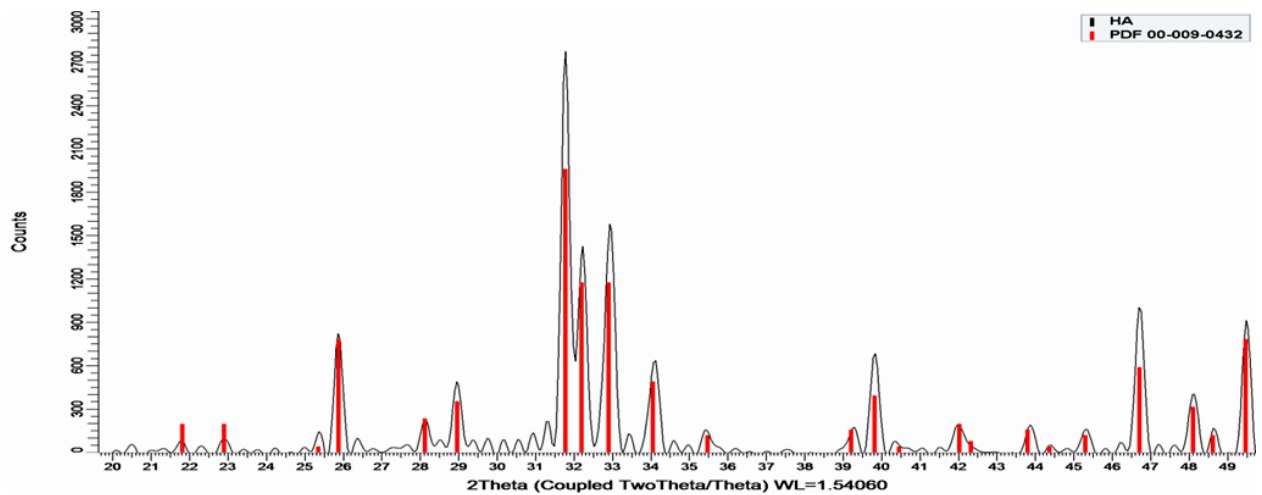
The results are stacked in the above graph where they can be compared with each other. OH group has highest intensity in HA. It is midway in HT and is almost nil in TCP. HABG does not show a peak corresponding to OH group and PG shows a broadened OH peak which may be attributed to the presence of moisture in it. Thus, it can be concluded that when silica group is present in the material, there is absence of OH peak. HA shows high intensity peaks which shows its crystalline structure. PG shows broadened peaks due to its amorphous nature. HABG is a combination of high peaks of HA and broad peaks of PG. No bands related to organic matter and incorporated water are seen.

4. X RAY DIFFRACTOMETRIC ANALYSIS

X-ray powder diffraction (XRD) is a rapid analytical technique primarily used for phase identification of a crystalline material and can provide information on unit cell dimensions. In this study, the test material was placed in an X ray diffractometer

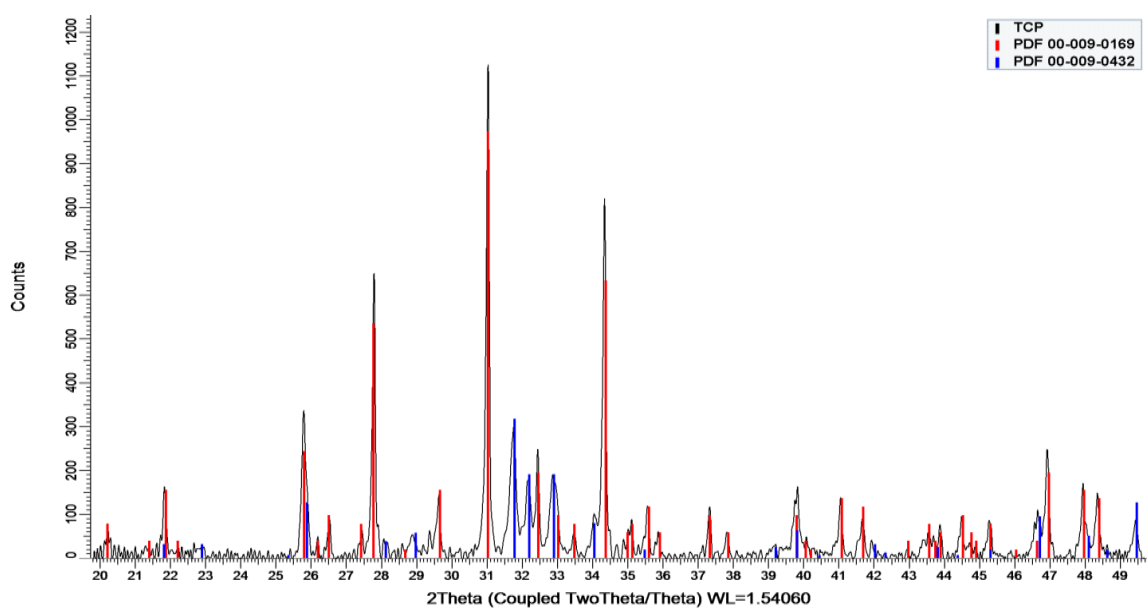
(Advance Bruker) and results were obtained. The 2θ range was between 20 and 50° , rate of heating of $2^\circ/\text{minute}$.

1. MONOPHASIC HYDROXY APAPTITE – Biograft HA



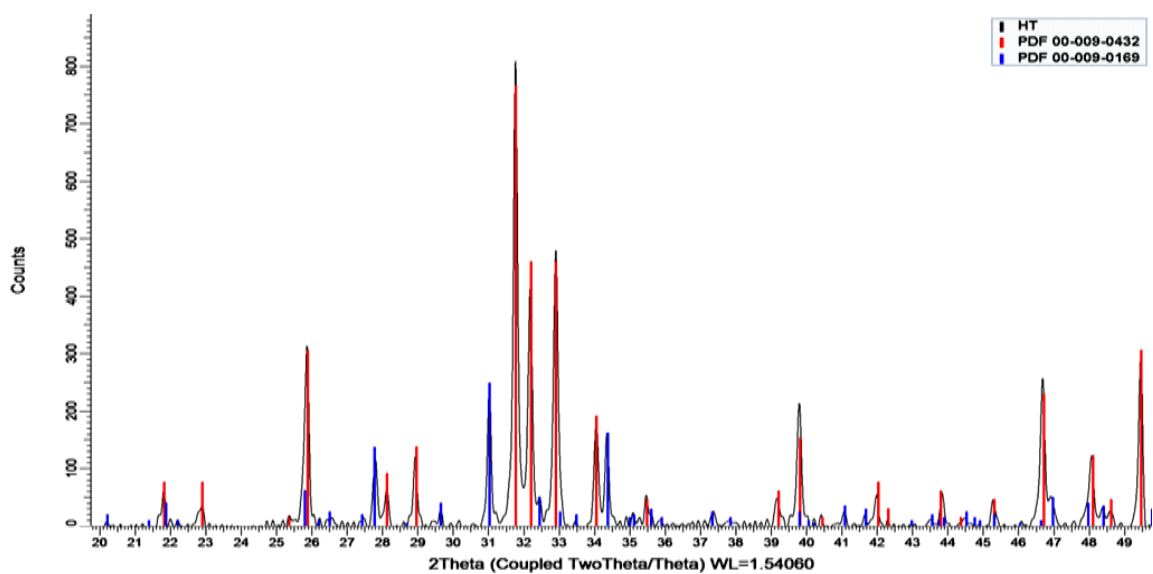
The highly and well defined peaks which are narrow show that HA is highly crystalline. The results fully match with every peak of the standard pattern.

2. TRICALCIUM PHOSPHATE – Biograft TCP



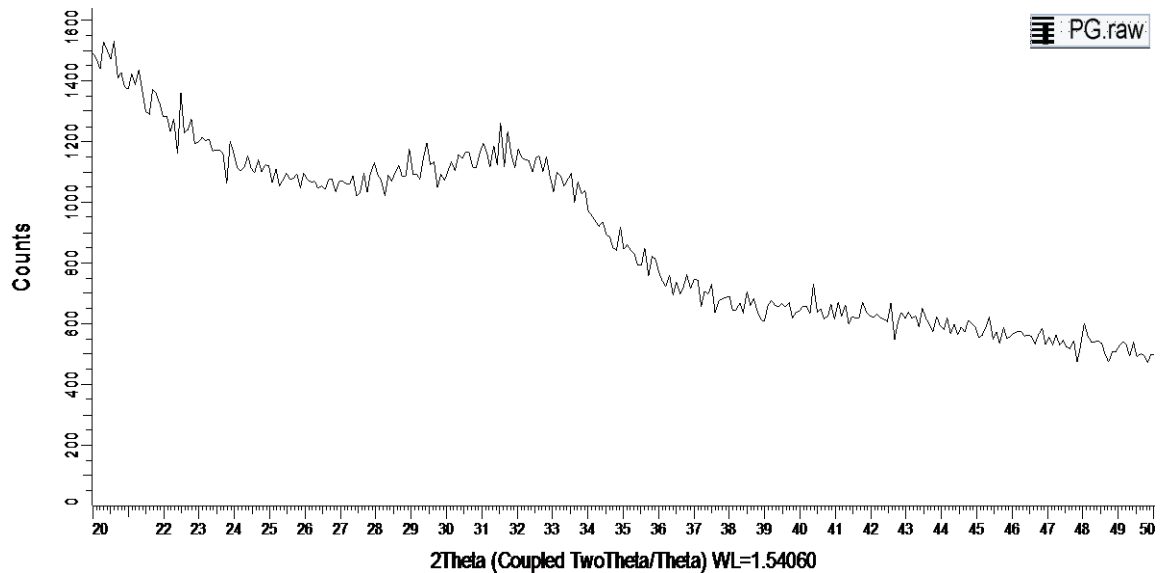
X ray diffractometry results show that the high peaks show a material with high crystallinity and small peaks show amorphous materials. In the present study, HA, HABG, TCP and HT show high peaks which have crystalline structure while PG shows broad peaks which are characteristic for amorphous materials. XRD data of TCP does not match fully with the standard. So it can be said that the material used in this study is not pure and it contains HA as its impurity. From the data, crystal size can be calculated and thus it can be concluded that crystallite size is increased and so solubility is reduced.

3. BIPHASIC HYDROXYAPATITE – Biograft HT



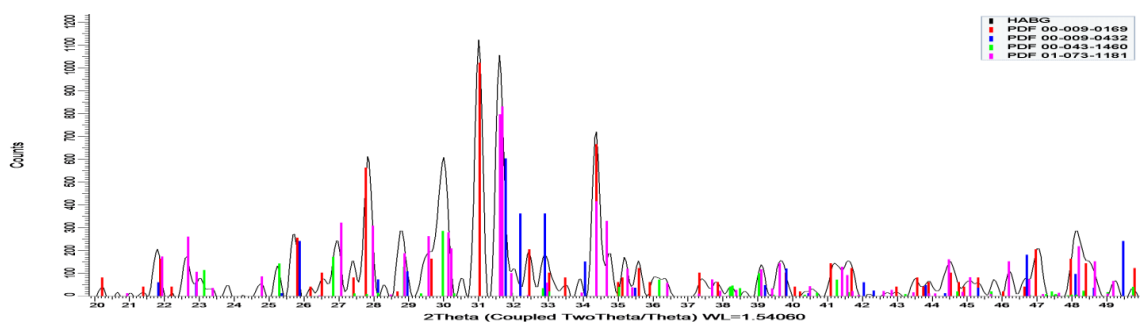
XRD data shows that the major phase here corresponds to HA.

4. BIOACTIVE GLASS - PERIOGLAS



PG is highly amorphous due to the numerous broad peaks seen and peaks are not fully resolved. This cannot be confirmed by XRD data as it is amorphous.

5. HYDROXYAPATITE BIOACTIVE GLASS COMBINATION -Biograft HABG



The highly and well defined peaks show that HABG is highly crystalline with peaks corresponding to HA, TCP and Calcitite and additionally this material shows amorphous nature as seen in the broad background. This confirms the presence of glass particles in HABG. The different phases seen in HABG are HA - 0432, TCP -

0169, CaSiO_3 (Wolastanite) - 1460, $\text{Ca}_5(\text{PO}_4)_2\text{SiO}_4$ (Calcium Phosphate Silicate) – 1181.

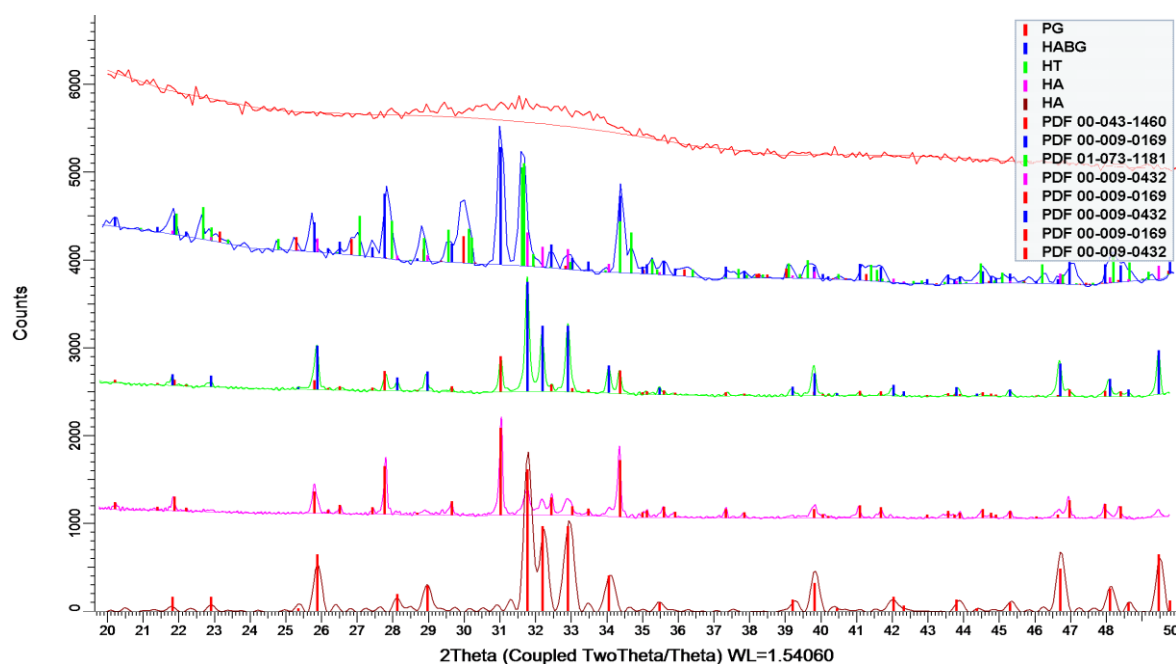
According to Scherrer equation, XRD data was used to find the crystal size.

The crystal size is shown in Table 3.

The crystallinity is shown in Table 4.

Material	Crystal size (nm)
HA	30-33
TCP	90-93
HT	69-72
HABG	33-37

Material tested	Crystallinity (%)
HA	90-93
TCP	87-90
HT	85-89
HABG	90-93

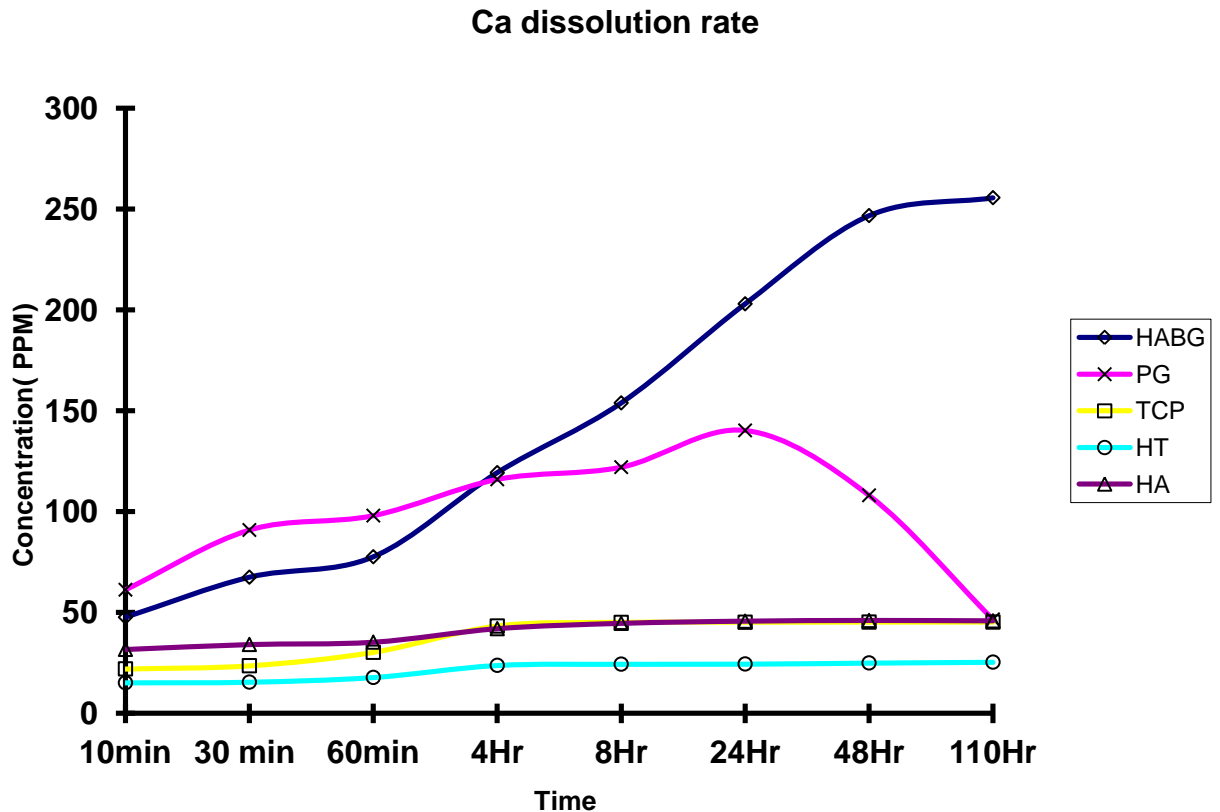


Stacked XRD data of 5 samples

XRD data is used to obtain lattice parameter information and also helps in identifying the mineralogical components of a substance. The stacked diagram helps to compare it with each other. Depending on the intensity of the peaks, crystallinity of the

material is assessed here. It can be concluded that the materials tested have crystallinity in the increasing order as – PG, HABG, TCP, HT and HA.

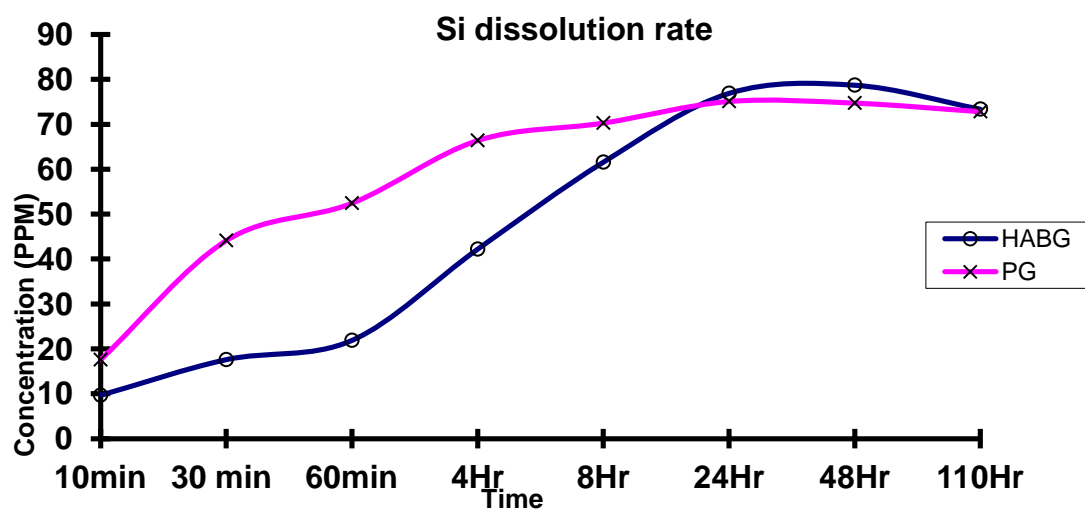
Dissolution rate of Calcium



Dissolution rate of Calcium is seen to increase in the 5 graft materials tested. Hydroxyapatite and Tri calcium phosphate combination shows dissolution at the same rate from 10 minutes upto 110 hours. It can be concluded that HT shows dissolution which is time independent. Tri calcium phosphate has increased dissolution than HT. Dissolution is seen to increase upto 4 hours but remains a constant after that. Hydroxyapatite shows slight dissolution till 4 hours and remains a constant after that. Perioglas shows dissolution to increase upto 24 hours but decreases after that. HABG also shows a constant rate of dissolution upto 48 hours but showed a slight saturation after that. Thus, it can be concluded from the present study that materials containing

hydroxapatite, tricalcium phosphate and its combination had less dissolution when compared to bioactive glass. Bioactive glass contains silica as its component and so it shows increased dissolution. Increased dissolution can be attributed to the increased silica content. It is said to be time dependent i.e. dissolution increases with time. The porous nature of PG is less and so it shows reduced solubility than HABG.

Dissolution rate of Silica



Perioglas shows increased dissolution rate for 24 hours and remains a constant after that. HABG shows increased dissolution upto 24 hours and decreases after that.

Discussion

Periodontal bone defects need to be filled with a biomaterial in order to obtain regeneration rather than healing by connective tissue formation. Autologous bone grafts are considered to be the “gold standard” in grafting materials, but their limited supply and donor site morbidity are major disadvantages. Allogenic and xenogenic bone grafts bear the risks of infection transmission and immune responses. This has led to the research and development of a wide range of alloplastic biomaterials including hydroxyapatite ceramics and bioactive glass ceramics. These biomaterials mimic the extracellular matrix of bone with respect to chemical composition as well as structural and functional properties. Many of these products are commercially available in India for use in periodontal bone grafting under different brand names. Manufacturers make tall claims with regard to their osteoconductive and bioactive potential, with no information being supplied on their actual physical and chemical properties.

The purpose of this work was to analyse and compare the physical and chemical characteristics of 5 commonly available alloplastic bone grafts which included calcium phosphates, mixed calcium phosphates, bioactive glass and a combined calcium phosphate – bioactive glass. The 3 fundamental parameters on which the biological performance of a biomaterial depends on are chemical composition, morphology and biodegradability. A thorough understanding of these properties is essential before their clinical application as they all influence the biological performance of the implanted graft material within the bone defect. A wide range of analytical methods were used to analyze these properties including scanning electron microscopy, thermogravimetry, infra-red spectroscopy, x ray diffractometry and dissolution tests.

An ideal synthetic bone substitute material should be (1) biocompatible promoting cell adhesion and proliferation, (2) exhibit mechanical properties that are comparable to the tissue being replaced, (3) have a porous 3 dimensional architecture that allows cell proliferation, vascularization and nutrient diffusion, (4) biodegradable at a preferred rate in order to be replaced by newly forming natural bone (5) allow easy manufacture and should be sterilizable.

Scanning electron microscopy of the biomaterial helps to assess grain size, porosity, surface irregularities and shape. Porosity of the biomaterial plays a decisive role for the behavior of cells especially osteoblasts. A sufficient pore size and an interconnecting pore structure is necessary for osteoblasts to grow into the graft. The particle size affects the contact area and also the packing characteristics of the materials which ultimately determines the macroporosity of the packed material which is crucial for bone regeneration. From the particle size related data, it is seen that PG and HA show smaller particles (100 – 300 μm) while TCP, HT and HABG show larger particles (200 – 500 μm). The particle sizes of the studied alloplasts are in accordance with studies that have shown that smaller particles (around 300 μm) are the basis for better performance when implanted into bone.⁵⁰ Studies have shown that very small particles (< 20 μm) elicit more inflammation than large particles (50 – 350 μm)⁴⁹. Surface roughness is known to influence the cell attachment in vitro and in vivo. Studies show that irregularly shaped particles produced a greater response than spherical particles.⁵¹ Rough apatitic structures enhance osteoclastic attachment compared with smooth ones.⁵² In the present study Biograft HA, Biograft TCP and Biograft HABG showed rough and irregular surface, while Perioglas and Biograft HT showed a smooth surface. These surface characteristics are a result of the sintering process and presence of glass structure.

With respect to the effect of porosity on bone regeneration, there is difference of opinion in published literature. The ideal pore size for a bioceramic should approximate that of bone. Studies have shown that microporosity (diameter < 10 μm) allows body fluid circulation whereas macroporosity (diameter > 100 μm) provides a scaffold for bone – cell colonization and is said to enhance new bone formation as they allow the migration and proliferation of osteoblasts and mesenchymal cells. Studies show that the presence of microporosity might alter the pattern and dynamics of osteointegration and enhance ionic exchange with body fluids. Nanoporous structure improves cell adhesion, proliferation and differentiation.⁵³⁻⁵⁴ SEM data of pore size of tested material shows that with the exception of PG all other alloplasts show porous architecture. The surface of perioglas is said to be smooth with less roughness and is due to the presence of glass with no pores visible. Biograft HT shows smooth and sintered surface particles with nano pores visible. All the other materials show rough surface with the presence of micro and nano sized pores ranging from 0.5 – 1 μm . In the present study as all the samples except Perioglas are in granular form pore interconnectivity is naturally ensured. The results confirm that the materials tested except Perioglas are within the recommended range for pore size in literature.

Thermogravimetric analysis is used to determine the content of water, organic material (like collagen) and mineral (CaP). For all of the alloplasts in our study only a minimal weight loss upto 2 % was seen which can be attributed to the presence of moisture or due to oxidation of the samples. As all the test materials were synthetic or alloplastic, there was the absence of lattice water or organic content. All the tested materials were stable upto 1000° C, which renders all test materials to be thermally stable and phase pure without any impurities.

Infra red analysis shows the presence of main functional groups such as phosphates and carbonates. The calcium phosphate class of materials (HA, TCP and HT) and HABG showed almost similar stretching and vibration patterns for both functional groups. Phosphate peak was broad in Perioglas which may be due to the amorphous nature of the material. In the Infrared spectra data from the 5 tested materials, hydroxyl peaks had highest intensity in HA, with midway values in HT and almost nil in TCP. HABG does not show a peak corresponding to OH group and PG shows a broadened peak which may be attributed to the presence of moisture in it. Thus it can be concluded that when silica group is present in the material, there is absence of hydroxyl peak. HA shows high intensity peaks which shows its crystalline structure. PG shows broadened peaks due to its amorphous nature. HABG is a combination of high peaks of HA and broad peaks of PG. No bands related to organic matter or incorporated water was seen. Studies have shown that an apatite layer forms on the ceramic surface when implanted. This layer consists of carbonate-ion-containing apatite which forms a bond with human bone. Carbonated apatite are resorbed by osteoclasts. It has been suggested that the carbonate content may stimulate the carbonic anhydrase activity known to promote the osteoclastic acidic secretion in vitro.⁵⁶ The results obtained in the present study are similar to those obtained by Tadic et al in 2004 in which HA based ceramics show calcium phosphate bands in a sharp and split way indicative of high crystallinity.²⁶

X ray diffraction patterns of the 5 alloplastic materials indicate their chemical composition (presence of crystalline phases) and lattice parameter information. The XRD peaks of the samples were well defined. Among the 5 alloplastic materials, HA, HABG, TCP and HT showed typical crystalline structure whereas PG showed broad peaks indicating the amorphous nature of the material. An increasing order of

crystallinity was obtained from XRD data as PG, HABG, TCP, HT and HA. If the crystallite size of HAP ceramics is very small and if there is carbonate incorporated the biodegradation is strongly enhanced due to a higher solubility. The degree of crystallinity affects the solubility behavior of apatites. Highly crystalline apatites (HA) tend to be very insoluble, while poorly crystalline apatites (TCP) tend to have higher relative solubilities.⁴¹

The commonly proposed mechanism of bioactivity of HA involves the dissolution of calcium and phosphate ions from HA. This process within the body is mediated through the extracellular fluid environment and osteoclastic action. Dissolution releases increased concentrations of calcium and inorganic phosphate in the space between the bone graft and existing bone. Precipitation of HA into this space will result in incorporation of bone graft into the existing bone.⁵⁷ The presence of small fragments of bone graft creates problems in the preferential gathering of cellular degradation elements, the decomposition of such fragments can obstruct the interparticle spaces among graft particles leading to delayed bone formation.²¹ Many calcium phosphate based materials have been used in the preparation of porous scaffolds whose Ca / P ratio has been modified to produce varying compounds like hydroxyapatite (Ca / P ratio = 1.67), tricalcium phosphate (Ca / P ratio = 1.5) and biphasic products. Biomaterials with a low Ca / P ratio resorb more rapidly, giving rise to unpredictable biodegradation profiles and resulting in undesirable loss of mechanical strength. While those with greater Ca / P ratios degrade more slowly but may give rise to remnants that can induce inflammation and also less new bone formation around the scaffold. The combination of different calcium phosphate products can be used as a strategy to control resorption rates. Among the material tested in the present study biphasic hydroxyapatite and HABG are examples of

combination grafts. Factors that affect the solubility of a material include the method of preparation, the resultant crystallinity and density and the extent of ionic substitutions into the apatite lattice. These ionic substitutions disrupt the structure of lattice. Ionic substitutions such as carbonate have been shown to increase the solubility of apatites. Studies have shown the presence of silicon in vivo within active calcification sites demonstrates its critical role in the bone calcification process.⁵⁸

In the dissolution tests done for calcium in the 5 alloplastic biomaterials, all the materials showed positive results. Bioactive glass class of grafts (PG and HABG) had more dissolution when compared to hydroxyapatite class (HA, TCP and HT), this finding can be explained by the fact that bioactive glass contains silica as its component and it shows increased dissolution which was time dependent. Another interesting finding of this study was that among the hydroxyapatite class of materials HT had less dissolution when compared to TCP and HA. This might be attributed to the differences in particle size which had been earlier confirmed by SEM studies. The decreased dissolution of HA can be attributed to the high crystalline nature of the material which was confirmed by XRD. Legeros et al in 2003 mentioned about the adjusting of degradation kinetics of calcium phosphates especially in large defects by combining a highly soluble phase (TCP) with a non soluble phase (HA) to create biphasic ceramics.³⁶ In the present study, HT showed slower resorption rate than both HA and TCP which may be due to an increased HA/ TCP ratio. Hydroxyapatites manufactured by the sintering process have been shown to be biodegradable but at a very slow rate. The factors during manufacture which affect dissolution include the sintering temperature, the duration of sintering and the Ca / P ratio in the feed material²³. β TCP ceramics are faster degradable than HAP ceramics.

There are 2 methods of *in vivo* degradation of calcium phosphate bioceramics: osteoclastic activity and dissolution process which depends on the nature of the biomaterial. The release of calcium ions from the biomaterial plays a critical role in osteoclastic activity and above a critical range of calcium ion levels, osteoclastic resorption is inhibited. Other factors which influence osteoclastic activity is structure of ceramic and crystallinity.⁵⁹

The second dissolution test was done for silica, the bioactive glass group of material (PG and HABG) which are silica based were tested. Both PG and HABG showed increased dissolution of silica upto 24 hours, with PG showing constant values and HABG showing decreasing rates after 24 hours. The dissolution of silica from bioactive glasses is an important step in its increased bioactivity properties. Direct bonding to bone has been reported with the formation of a carbonate substituted hydroxyapatite like (HCA) layer on the glass surface. This layer is similar to the mineral constituent of bone. The first stage in this process is the hydrolysis of silica from the biomaterial and creation of silanol groups on glass structure. These unique reactions of bioactive glass has lead to it being reported as having osteoinductive as well as osteoconductive properties. Dissolution affects the osteoconductivity of the material. In a healthy site, where rapid regeneration is expected, it is advisable to use a silica based material whereas in a pathogenic condition, a material with slowed resorption can be used. From the present study we can conclude that hydroxyapatite based materials like HA, HT and TCP can be used in the treatment of pathogenic conditions. The results obtained in this study are similar to those obtained by Tadic et al in 2004 who did a physicochemical characterisation of 14 different calcium phosphate based bone substitution materials.²⁶

The bioactivity of alloplastic materials depends on many factors during the synthesis procedure, such as precursor reagents, impurity contents, crystal size and morphology, concentration and mixture order of reagents, pH and temperature. One of the major limitations of this study is our lack of knowledge of the synthesis procedure of these 5 alloplastic biomaterials. A deeper correlation with the physicochemical characters could have been elucidated if the manufacturing method of these biomaterials were known. Another drawback noticed was that as many of the alloplasts had nano sized pores and microporosity, further quantitative investigation of porosity could have been done. For this mercury intrusion porosimetry should have been done. Inductively coupled plasma optical atom emissions spectroscopy [ICP-OES] is used to analyze the ceramic for elements like calcium, copper, iron, chromium and phosphorous. This data can be utilized to calculate Ca/ P ratio, which affects many properties of the material. This test was not done in the present study. The dissolution analysis done in the present study was in a closed system, where there is the possibility of the material contents coming into equilibrium with its dissolved ions in the solution surrounding the mineral. These results cannot be fully used to describe in vivo performance of the alloplastic material as the in vivo dissolution occurs in a thermodynamically open system.

Summary & Conclusion

The main objective of present work was the physicochemical characterization of 5 commercial sample of alloplasts used for bone grafting. The alloplastic biomaterials belonged to 3 main classes calcium phosphate group (HA, TCP and HT), bioactive glass group (PG) and a combination graft (HABG). However even for those with similar chemical characteristics, significant differences were noted with regard to particle size, porosity, surface roughness, presence of functional groups, crystallinity and dissolution properties. Among the materials tested calcium phosphate based ceramics and bioactive glass – ceramic combination showed porous surface architecture parameters conducive to cellular and vascular proliferation. Thermogravimetric analysis revealed that all the materials were phase pure with no impurities. Infra red spectrometry showed presence of functional groups essential for bone integration in all test materials with Perioglas and Biograft HABG showing presence of silica which has a beneficial effect in bone formation. X ray diffractometry data revealed that with the exception of Perioglas which was amorphous all the other materials were crystalline in nature. Increased dissolution of calcium and silica were seen in bioactive glass group when compared with calcium phosphate and mixed calcium phosphate grafts. Calcium phosphate ceramics have osteoconductive properties while bioactive glasses are reported to be both osteoinductive as well as osteoconductive. Next-generation biomaterials should combine bioactive and bioresorbable properties to activate in vivo mechanisms of tissue regeneration, stimulating the body to heal itself and leading to replacement of the scaffold by the regenerating tissue.

Bibliography

1. **Carranza, Newman, Klokkevold** *Carranza`s Clinical Periodontology* – Elsevier Tenth Edition, Pages 45 -85
2. **Jaebum Lee, Andreas Stavropoulos, Crisitiano Susin, Ulf M. E. Wikesjo**, Periodontal Regeneration : Focus of Growth and Differentiation Factors *Dental Clinics of North America* 54(2010)93-111
3. **Melcher, A.H. and J.E. Eastoe**. 1969. The connective tissues of the periodontium. In: A.H. Melcher and W.H. Bowen (eds.), *Biology of the periodontium*. Academic Press, New York, ~167-328.
4. **Williams, D.M., F.J. Hughes, E.W. Odell and P.M. Farthing**. 1992a. The normal periodontium. In: *Pathology of periodontal diseases*. Oxford university press, New York, pp: 17-30.
5. **Genco, RJ**. 1990. Pathogenesis and host response in periodontal disease. In: Genco R.J., H.M. Goldman and D.W. Cohen (eds.), *Contemporary periodontics*. C.V. Mosby, Toronto, pp. 184-193.
6. **Zambon, J.J**. 1990. Microbiology of periodontal disease. In R.J. Genco, H.M. Goldman, and D.W. Cohen (eds.), *Contemporary periodontics*. C.V. Mosby, St. Louis, p147-160
7. **Jan Lindhe, Niklaus Lang, Thorkild Karring** - Clinical Periodontology and Implant Dentistry: Blackwell 5 th Edition
8. **Raul G. Caffesse' Carlos R. Quiñones** Polypeptide growth factors and attachment proteins in periodontal wound healing and regeneration *Periodontology 2000 Volume 1, Issue 1, pages 69–79, February 1993*
9. **Cobb CM**. Non-surgical pocket therapy. *Ann Periodontol* 1996: 1: 443–490.

10. **Noel Claffey, Ioannis Polyzois & Paraskevi Ziaka** An overview of nonsurgical and surgical therapy *Periodontology 2000, Vol. 36, 2004, 35–44*
11. American Academy of Periodontology Glossary of Periodontal Terms -3rd Edition 1992, Chicago : *American Academy of Periodontology*
12. **Rosenberg E., H DipDent, and Rose L.F:** Biologic and clinical considerations for autografts and allografts in periodontal regeneration therapy: *Dent Clin North Am 1998; 42; 3; 467-488*
13. **Schallhorn RG.** Present status of osseous grafting procedures. *J Periodontol 1977; 48: 570-576.*
14. **Aichelmann-Reidy M.E. and Yukna R.A.:** Bone replacement grafts: *Dent Clin North Am 1998; 42; 3; 491-503*
15. **Mats Hallman & Andreas Thor** Bone substitutes and growth factors as an alternative / complement to autogenous bone for grafting in implant dentistry *Periodontology 2000, Vol. 47, 2008, 172–192*
16. **Hisham F. Nasr, Mary Elizabeth Aichelmann-Reidy, Raymond A. Yukna** *Periodontology 2000 Volume 19, Issue 1, pages 74–86, February 1999*
17. **Kurz LT, Garfin SR, Booth RE Jr.** Harvesting autogenous iliac bone grafts. A review of complications and techniques. *Spine (Phila Pa 1976). 1989 Dec;14(12):1324-31.*
18. **William R. Moore, Stephen E. Graves and Gregory I. Bain** Synthetic Bone Graft Substitutes *Anz J. Surg. (2001) 71, 354–361*
19. **Edward S Cohen** Atlas of cosmetic and reconstructive periodontal surgery, 3rd Edition
20. **Bernard G.W:** Healing and repair of osseous defects: *Dent Clin North Am 1991; 35; 3; 469-477.*

21. **M. Fabbri, G.C. Celotti and A. Ravaglioli** Hydroxyapatite-based porous aggregates: physico-chemical nature, structure, texture and architecture *Biomaterials* 16 (1995) 225-228
22. **S. Best, B. Simt, M. Kaysert, S. Downest** The dependence of osteoblastic response on variations in the chemical composition and physical properties of hydroxyapatite *Journal Of Materials Science: Materials In Medicine* 8 (1997) 97 –103
23. **S. Joschek, B. Nies, R. Krotz, A. GoK pferich** Chemical and physicochemical characterization of porous hydroxyapatite ceramics made of natural bone *Biomaterials* 21 (2000) 1645-1658
24. **R. M. Pilliar, M.J. Filiaggi, J.D. Wells, M.D. Grynepas, R.A. Kandel** Porous calcium polyphosphate scaffolds for bone substitute applications in vitro characterization *Biomaterials* 22 (2001) 963-972
25. **A.E. Porter, N. Patel, J.N. Skepper, S.M. Best, W. Bonfield** Comparison Of In Vivo Dissolution Processes In Hydroxyapatite And Silicon-Substituted Hydroxyapatite Bioceramics *Biomaterials Volume 24, Issue 25, November 2003, Pages 4609–4620*
26. **Tadic D, Epple M.** A thorough physicochemical characterisation of 14 calcium phosphate-based bone substitution materials in comparison to natural bone. *Biomaterials*. 2004 Mar;25(6):987-94.
27. **Luna-Zaragoza, E. T. Romero-Guzmán and L. R. Reyes-Gutiérrez** Surface and Physicochemical Characterization of Phosphates Vivianite, $\text{Fe}_2(\text{PO}_4)_3$ and Hydroxyapatite, $\text{Ca}_5(\text{PO}_4)_3\text{OH}$ D. *Journal of Minerals & Materials Characterization & Engineering*, Vol. 8, No. 8, pp 591-609, 2009

28. **Lidia A. Sena, Mirta M. Caraballo, Alexandre M. Rossi, Gloria A. Soares** Synthesis and characterization of biocomposites with different hydroxyapatite–collagen ratios *J Mater Sci: Mater Med* (2009) 20:2395–2400
29. **Laura Floroian** Biocompatibility And Physical Properties Of Doped Bioactive Glass Ceramics *Bulletin Of The Transilvania University Of Brasov Vol. 3 (52) – 2010*
30. **O. M. Goudouri, E. Kontonasaki, A. Theocharidou, L. Papadopoulou, X. Chatzistavrou, P. Koidis, and K. M. Paraskevopoulos** In Vitro Bioactivity Studies of Sol-Gel Derived Dental Ceramics/Bioactive Glass Composites in Periodically Renewed Biomimetic Solution *Bioceramics Development and Applications Vol. 1 (2011)*
31. **Azadeh Rezakhani and M. M. Kashani Motlagh** Synthesis and characterization of hydroxyapatite nanocrystal and gelatin doped with Zn²⁺ and cross linked by glutaraldehyde *International Journal of Physical Sciences Vol. 7(20), pp. 2768 - 2774, 23 May, 2012*
32. **Fabian Peters, Karsten Schwarz, Matthias Epple** The structure of bone studied with synchrotron X-ray diffraction, X-ray absorption spectroscopy and thermal analysis *Thermochimica Acta Volume 361, Issues 1–2, 3 October 2000, Pages 131-138*
33. **Suchanek WL, Shuk P, Byrappa K, Riman RE, TenHuisen KS, Janas VF** Mechanochemical hydrothermal synthesis of carbonated apatite powders at room temperature *Biomaterials. 2002 Feb;23(3):699-710*
34. **Suchanek WL, Byrappa K, Shuk P, Riman RE, Janas VF, TenHuisen KS.** Preparation of magnesium-substituted hydroxyapatite powders by the mechanochemical-hydrothermal method *Biomaterials. 2004 Aug;25(19):4647-57.*
35. **Susan I, Fumio Watari, Motohiro Uo, Shoji Okhawa, Kazuchika Tamura, Wei Wang, Fuzhai Cui** The preparation and characteristics of a carbonated hydroxyapatite/ collagen

-
- composite at room temperature *J Biomed Mater Res Part B: Appl Biomater* 74B:817-821,2005
36. **R.Z Legeros, S. Lin, R. Rohanzadeh, D. Mijares, J. P. Legeros** Biphasic calcium phosphate bioceramics: preparation, properties and applications *Journal of Materials Science:Materials in Medicine* 14(2003)201-209
37. **David C. Greenspan** Comparison Of A Synthetic And Bovine Derived Hydroxyapatite Bone Graft Substitute 2011
38. **Esther Garcí'a-Tunõ'n, Ramiro Couceiro, Jaime Franco, Eduardo Saiz, Francisco Guitia'n** Synthesis and characterisation of large chlorapatite single-crystals with controlled morphology and surface roughness *J Mater Sci: Mater Med* 2012
39. **Masayuki Okazaki, Junzo Takahashi, and Hiroshi Kimura** Crystallinity, solubility, and dissolution rate behavior of fluoridated CO₃ apatites *Journal of Biomedical Materials Research, Vol. 16*,851-860 (1982)
40. **H. C. Gledhill, I.G. Turner, C. Doyle** In vitro dissolution behaviour of two morphologically different thermally sprayed hydroxyapatite coatings *Biomaterials* 22 (2001) 695-700
41. **Mark T. Fulmer, Ira C. Ison, Christine R. Hankermayer, Brent R. Constantz,John Ross** Measurements of the solubilities and dissolution rates of several hydroxyapatites *Biomaterials Volume 23, Issue 3, February 2002, Pages 751–755*
42. **K. Franks, I. Abrahams¹, J. C. Knowles** Development Of Soluble Glasses For Biomedical Use Part I: In Vitro Solubility Measurement *Journal Of Materials Science: Materials In Medicine* 11 (2000) 609±614

43. **Christine R. Hankermeyera, Kevin L. Ohashi, David C. Delaney, John Ross, Brent R. Constantz** Dissolution rates of carbonated hydroxyapatite in hydrochloric acid *Biomaterials* 23 (2002) 743–750
44. **M. Nilsson, J-S. Wang, L. Wielanek, K. E. Tanner, L. Lidgren** Biodegradation And Biocompatibility Of A Calcium Sulphate-Hydroxyapatite Bone Substitute *The Journal Of Bone And Joint Surgery Vol. 86-B, No. 1, January 2004*
45. **Xia Li, Atsuo Ito, Yu Sogo, Xiupeng Wang, and R.Z. LeGeros** Solubility of Mg-containing β -tricalcium phosphate at 25 °C *Acta Biomater.* 2009 January ; 5(1): 508–517
46. **H. Y. Yang, I. Thompson, S. F. Yang, X. P. Chi, J. R. G. Evans, R. J. Cook** Dissolution characteristics of extrusion freeformed hydroxyapatite–tricalcium phosphate scaffolds *J Mater Sci: Mater Med* (2008) 19:3345–3353
47. **Weilie Zhon and Zhong Liu Wang** Scanning Microscopy for Nano technology – Techniques and Applications ,Pages 1- 39
48. Polymer synthesis and characterization – A Laboratory Manual :**Stanley R. Sandler**, Pages 98 - 108
49. **M. Birholz** Thin film analysis by X ray scattering, Pages 1- 41
50. **Cruz A, Pochapski M, Daher J.** Physico-chemical characterization and biocompatibility evaluation of hydroxyapatites. *J Oral Sci* 2006;48:219-226.
51. **Jui-Sheng Sun, Hwa Chang Liu, Walter Hing-Shong.** Influence of HA particle size on bone cell activities : an in vitro study. *J. Biomed Mater Res* 39, 390-97
52. **Gomi K, Lowenberg B, Shapiro G, 1993.** Resorption of sintered synthetic hydroxyapatite by osteoclasts in vitro. *Biomaterials*, 14: 91-96.

53. **Ravaglioli, A. Krajewski.** “Bioceramics: materials, properties, applications”. (Chapman and Hall, London, 1992) p. 432
54. **Karageorgiou V, Kaplan D.** Porosity of 3D biomaterial scaffolds and osteogenesis. *Biomaterials* 2005;26:5474-5491.
55. **Hing KA, Annaz B, Saaed S, Revell PA.** Micro-porosity enhances bioactivity of synthetic bone graft substitutes. *J Mater Sci: Mater Med* 2005;16:467-475.
56. **Doi Y, Iwanaga H, Shibutani T. 1999.** Osteoclastic responses to various calcium phosphates in cell cultures. *J Biomed Mater Res*, 47: 424-33
57. **Weng J, Liu Q, Wolke JGC, Zhang X.** formation and characteristics of the apatitic layer on plasma sprayed HA coatings in simulated body fluids. *Biomaterials* 1995;18:1027-1035
58. **Carlisle EM. Silicon:** a possible factor in bone calcification. *Science* 1970;167: 279-80.
59. **De Bruijn JD, Bovell YP, Davies JE. 1994.** Osteoclastic resorption of calcium phosphates is potentiated in postosteogenic culture conditions. *J. Biomed Mater Res*, 28:105-12.
-